J|A|C|S
ARTICLES
Published on Web 06/07/2006

An Approach to Helical Tubular Self-Aggregation Using C_2-Symmetric Self-Complementary Hydrogen-Bonding Cavity Molecules

Sigitas Stončius,[†] Edvinas Orentas,[†] Eugenius Butkus,*[,†] Lars Öhrström,[‡] Ola F. Wendt,[¶] and Kenneth Wärnmark*[,¶]

Contribution from the Department of Organic Chemistry, Vilnius University, Naugarduko 24, LT03225 Vilnius, Lithuania, Department of Chemical and Biological Engineering, Physical Chemistry, Chalmers University of Technology, SE-41296 Göteborg, Sweden, and Organic Chemistry, Department of Chemistry, Lund University, P.O. Box 124, SE-22100 Lund, Sweden

Received February 27, 2006; E-mail: kenneth.warnmark@organic.lu.se; eugenijus.butkus@chf.vu.lt

Abstract: In an approach to helical self-aggregation, C_2-symmetric cavity compounds based on the fusion of the bicyclo[3.3.1]nonane and indole framework and incorporating two 2-pyridone hydrogen-bonding motifs, compounds (−)-**4** (pyrrole *N*-butyl) and (−)-**5** (pyrrole *N*-decyl), have been synthesized. The 2-pyridone AD−DA hydrogen-bonding motif failed to operate in the solid state as demonstrated by X-ray diffraction analysis of (−)-**4**. Instead, the hydrogen-bonded (D−A) chains ···O═C−N−H···O═C−N−H···O═C−N−H···, interconnecting columnar stacks, comprise helices of the right-handed (P) chirality motif. In solution, the aggregation of (−)-**5** was studied by NMR, electronic, and CD spectroscopies, and VPO measurements. These investigations strongly suggest that (−)-**5** associates to oligomers in $CHCl_3$ and CH_2Cl_2 using the 2-pyridone motif, fitting the equal *K* model, and that π-stacking can be ruled out as a mode of aggregation. We conclude that the so formed aggregates of (−)-**5** have a helical structure, based on the fact that only helical tubular structures can result when enantiomerically pure **5** uses its 2-pyridone AD−DA hydrogen-bonding motifs for aggregation.

Introduction

Tubular structures are important modules in the engineering of functional nano-objects, such as nanowires, molecular tubes, and flow-through reactors, due to their defined inner and outer surfaces and termini as well as their unidirectional propagation. Organic nanotubes are particularly interesting for molecular engineering because, by constructing them using organic synthesis, their properties can be more or less tailor-made. There are several general approaches for the design of organic nanotubes, such as hollow helices, rods self-assembled to hollow tubular spaces, stacked rings and rosettes, and wedged disks.[1] In approaches toward molecular tubes based on covalent backbones, helical linear aggregates (supramolecular oligo- and polymers) with a hollow interior constitute an important class of compounds as exemplified by extended phenylene helicenes and foldamers as well as by structures owing their helicity to intramolecular hydrogen bonding, intramolecular covalent cross-linking, or the 2,2′-bipyridine helicity codon.[2] Molecular tubes based on noncovalent aggregation do exist in Nature. The most prominent examples are the transmembrane ion channel peptide Gramicidin A, the coating of the tobacco mosaic virus by noncovalently assembled peptides, and the formation of microtubules involving noncovalent helical backbones.[3] There are many synthetic examples of helical tubular structures based on noncovalent aggregation; however, most of them are found in the solid state.[4] Examples where such structures have been proven outside the solid state are based on either formation of the helical backbone by π-stacking of mesogens, exemplified by Katz's hexahelicenequinone,[5] Lehn's oligopyridine−pyridazine strands,[6] and Moore's oligo-(*m*-phenylene-ethynylene) foldamers,[7] or by hydrogen bonding stabilized either by

[†] Vilnius University.
[‡] Chalmers University of Technology.
[¶] Lund University.

(1) (a) Balbo Block, M. A.; Kaiser, C.; Khan, A.; Hecht, S. *Top. Curr. Chem.* **2005**, *245*, 89−150. (b) Bong, D. T.; Clark, T. D.; Granja, J. R.; Ghadiri, M. R. *Angew. Chem., Int. Ed.* **2001**, *40*, 988−1011. (c) Cornelissen, J. J. L. M.; Rowan, A. E.; Nolte, R. J. M.; Sommerdijk, N. A. J. M. *Chem. Rev.* **2001**, *101*, 4039−4070. (d) Nakano, T.; Okamoto, Y. *Chem. Rev.* **2001**, *101*, 4013−4038.

(2) For leading references, see: (a) Han, S.; Bond, A. D.; Disch, R. L.; Holmes, D.; Schulman, J. M.; Teat, S. J.; Vollhardt, K. P. C.; Whitener, G. D. *Angew. Chem., Int. Ed.* **2002**, *41*, 3223−3227. (b) Nelson, J. C.; Saven, J. G.; Moore, J. S.; Wolynes, P. G. *Science* **1997**, *277*, 1793−1796. (c) De Santis, P.; Morosetti, S.; Rizzo, R. *Macromolecules* **1974**, *7*, 52−58. (d) Hamuro, Y.; Geib, S. J.; Hamilton, A. D. *Angew. Chem., Int. Ed.* **1994**, *33*, 446−468. (e) Hecht, S.; Kahn, A. *Angew. Chem., Int. Ed.* **2003**, *42*, 6021−6024. (f) Hanan, G. S.; Lehn, J.-M.; Kyritsakas, N.; Fischer, J. *J. Chem. Soc., Chem. Commun.* **1995**, 765−766.

(3) (a) Langs, D. A. *Science* **1988**, *241*, 188−191. (b) Ketchem, R. R.; Hu, W.; Cross, T. A. *Science* **1993**, *261*, 1457−1460. (c) Klug, A. *Angew. Chem., Int. Ed.* **1983**, *95*, 565−582. (d) Noagles, E. *Annu. Biophys. Biomol. Struct.* **2001**, *30*, 397−420.

(4) Bishop, R.; Dance, I. G. *Top. Curr. Chem.* **1988**, *149*, 137−188.

(5) Lovinger, A. J.; Nuckolls, C.; Katz, T. J. *J. Am. Chem. Soc.* **1998**, *120*, 264−268.

(6) Cuccia, L. A.; Lehn, J.-M.; Homo, J.-C.; Schmutz, M. *Angew. Chem., Int. Ed.* **2000**, *39*, 233−237.

(7) Prest, P.-J.; Prince, R. B.; Moore, J. S. *J. Am. Chem. Soc.* **1999**, *121*, 5933−5939.

10.1021/ja061160z CCC: $33.50

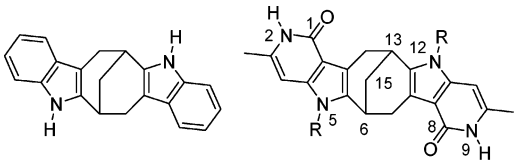

1

(-)-(6*R*,13*R*)-**3**: R = H
(-)-(6*R*,13*R*)-**4**: R = C_4H_9
(-)-(6*R*,13*R*)-**5**: R = $C_{10}H_{21}$

Figure 1. Cavity compounds based on the fusion of bicyclo[3.3.1]nonane and (aza)indole skeletons. The diindole compound **1** and bis(4-oxo-5-azaindole) analogues designed for helical tubular self-aggregation **3**−**5**.

Scheme 1

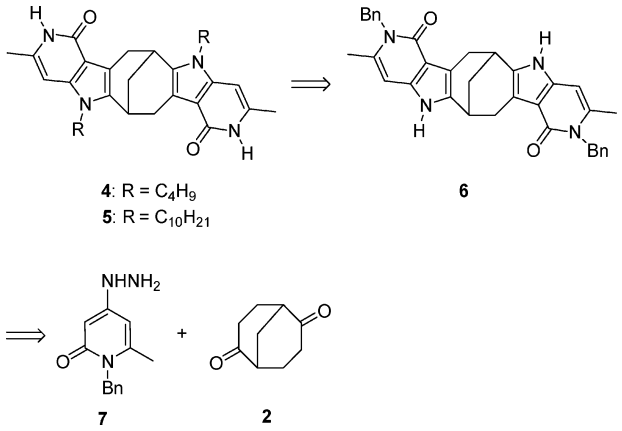

4: R = C_4H_9
5: R = $C_{10}H_{21}$

6

7

2

π-stacking, such as in Meijer's helical supramolecular polymer in water,[8] or hydrogen-bonding mesogens as exemplified by Lehn's tartaric acids containing bis(diaminopyridines) and di(uracil) moieties.[9]

In a quest for molecular tubular structures based on noncovalent helical backbones with no additional stabilization from liquid-crystalline properties or π stacking, the attention was drawn to rigid C_2-symmetric monomers with the possibility to associate end-to-end. An attractive class of such compounds is the chiral synthetic cavity molecules based on bicyclic ring systems[10] containing heteroatoms, such as Tröger's base, Kagan's ether, epiiminodibenzo[*b*,*f*][1,5]diazocine, and those based on the bicyclo[3.3.1]nonane framework, such as dibenzobicyclo[*b*,*f*][3.3.1]nona-5a,6a-diene, dibenzobicyclo[*b*,*f*][3.3.1]nona-5a,6a-diene-6,12-dione, bicyclo[3.3.1]nonane diquinoline, and bicyclo[3.3.1]nonane diquinoxaline.[11]

We have recently synthesized the C_2-symmetric cavity compound **1** based on the fusion of the bicyclo[3.3.1]nonane skeleton with indole framework (Figure 1), applying Fischer's indole synthesis on bicyclo[3.3.1]nonane-2,6-dione **2** (Scheme 1).[12] The cavity molecule **1** can be obtained conveniently in enantiomerically pure form due to the accessibility of optically pure **2**, readily obtainable by kinetic resolution of the racemate.[13]

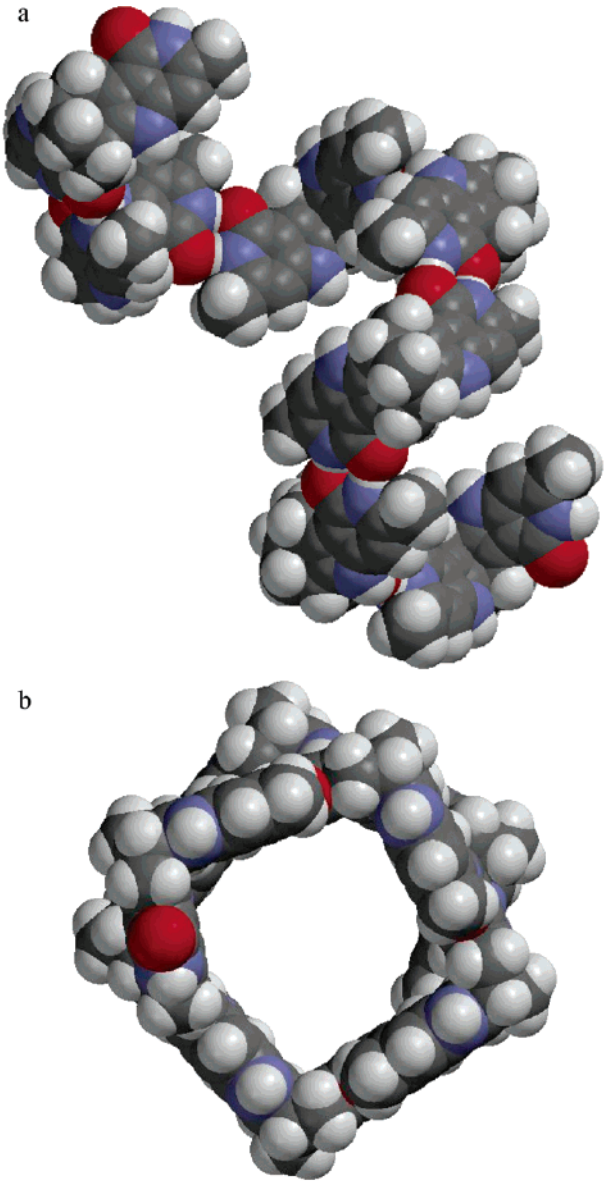

Figure 2. PM3-optimized[17] geometry of a proposed homochiral helical assembly of (6*S*,13*S*)-**3**. Side view (a) and top view (b).

By the incorporation of the self-complementary 2-pyridinone hydrogen-bonding AD−DA motif into **1** (A = acceptor, D = donor),[14] which is commonly employed in self-assembly processes in both solution and in the solid state,[15] we reasoned that the resulting structure, **3** (Figure 1),[16] in enantiomerically pure form, could be bound to assemble end-to-end, forming helical tubular structures. Molecular modeling by the semiempirical PM3 method (Figure 2),[17] using the hydrogen bonds of the 2-pyridone motif as the connector, suggests that the internal diameter of the proposed aggregate is ca. 12−14 Å. This is enough to host small organic molecules. Compound (±)-**3** is

(8) Brunsveld, L.; Vekemans, J. A. J. M.; Hirschberg, J. H. K. K.; Sijbesma, R. P.; Meijer, E. W. *Proc. Natl. Acad. Sci. U.S.A.* **2002**, *99*, 4977−4982.
(9) (a) Fouquey, C.; Lehn, J.-M.; Levelut, A.-M. *Adv. Mater.* **1990**, *2*, 254−257. (b) G.-Krzywicki, F.; Fouguey, C.; Lehn, J.-M. *Proc. Natl. Acad. Sci. U.S.A.* **1993**, *90*, 163−167.
(10) For recent reviews, see: (a) Valík, M.; Strongin, R. M.; Král, V. *Supramol. Chem.* **2005**, *17*, 347−367. (b) Turner, J. J.; Harding, M. M. *Supramol. Chem.* **2005**, *17*, 369−375.
(11) (a) Tröger, J. *J. Prakt. Chem.* **1887**, *36*, 225−245. (b) Kagan, J.; Chen, S. Y.; Adeppa, D. A., Jr.; Watson, W. H.; Zabel, V. *Tetrahedron Lett.* **1977**, *18*, 4469−4470. (c) Yamamoto, A. A. *J. Chem. Soc. C* **1968**, 1944−1949. (d) Prasad, R. S.; Roberts, R. M. *J. Org. Chem.* **1991**, *56*, 2998−3000. (e) Tatemitsu, H.; Ogura, F.; Nakagawa, Y.; Nakagawa, M.; Naemura, K.; Nakazaki, M. *Bull. Chem. Soc. Jpn.* **1975**, *48*, 2473−2483. (f) Rahman, A. N. M. M.; Bishop, R.; Craig, D. C.; Scudder, M. L. *Chem. Commun.* **1999**, 2389−2390. (g) Marjo, C. E.; Bishop, R.; Craig, D. C.; Scudder, M. L. *Eur. J. Org. Chem.* **2001**, 863−873.
(12) Butkus, E.; Berg, U.; Malinauskienė, J.; Sandström, J. *J. Org. Chem.* **2000**, *65*, 1353−1358.
(13) Hoffman, G.; Wiartalla, R. *Tetrahedron Lett.* **1982**, *23*, 3887−3888.
(14) The 2-pyridone hydrogen-bonding AD−DA motif corresponds to the 2-pyridone···2-pyridone $R_2^2(8)$ hydrogen-bonding synthon in graph set theory. See: (a) Etter, M. C.; MacDonald, J. C.; Bernstein, J. *Acta Crystallogr. B* **1990**, *46*, 256−262. (b) Bernstein, J.; Davis, R. E.; Shimoni, L.; Chang, N. L. *Angew. Chem., Int. Ed.* **1995**, *34*, 1555−1573.

soluble only in DMF and (−)-**3** in AcOH.[16] As a result, in the solid state, the solvent molecules competed with the 2-pyridone AD−DA self-complementary hydrogen-bonding motif, and the resulting aggregation of (±)-**3** and (−)-**3** failed to give the desired helical tubular structure as revealed by X-ray diffraction.[16] Instead, (±)-**3** forms hydrogen-bonded pleated band structures in which one of the 2-pyridone moiety of (±)-**3** interacts with the 2-pyridone moiety of a neighboring (±)-**3** via the AD−DA hydrogen-bonding pattern, while the carbonyl of the other 2-pyridone moieties of (±)-**3** acts as a hydrogen-bond acceptor of the pyrrole NH hydrogen in an adjacent molecule of (±)-**3** (the same is also observed for (−)-**3**). In addition, one molecule of DMF is hydrogen bonded to the remaining pyrrole NH hydrogen of (±)-**3**. Taking into consideration the results from the solid-state assembly of (±)-**3** and (−)-**3**, a second generation of compounds was designed in order to increase the chances that **3** would form helical tubular structures in the solid state and to facilitate the assembly in solution. We reasoned that attaching alkyl chains to the pyrrole nitrogens of **3** would increase the solubility in nonpolar solvents. That would increase the potential for aggregation using the 2-pyridone motif, necessary for the formation of tubular helical structures from the framework represented by **3**. In addition, alkylation of the pyrrole nitrogen atoms would also terminate the possibility for nonproductive pyrrole NH···O═C interactions between adjacent molecules.

Thus, enantiomerically pure pyrrole *N*-butyl and *N*-decyl derivatives of **3**, (−)-(6*R*,13*R*)-**4** and (−)-(6*R*,13*R*)-**5** (Figure 1) were synthesized, and the self-aggregation of (−)-**4** in the solid state and of (−)-**5** in solution was studied.

Results and Discussion

Synthesis. Numerous attempts to introduce alkyl chains regioselectively at the pyrrole nitrogens by direct alkylation of **3** with 1-bromodecane under typical conditions[18] in DMF with NaH as a base or in DMSO/KOH gave intractable mixtures of products. It is known that alkylation of 2-pyridone[19] itself, or 2(1*H*)-quinolones,[20] azaindoles, and related systems,[21] leads to mixtures of products depending on structural features and reaction conditions. Keeping in mind that **3** contains six possible nucleophilic centers in total, this synthetic route was abandoned.

Scheme 2[a]

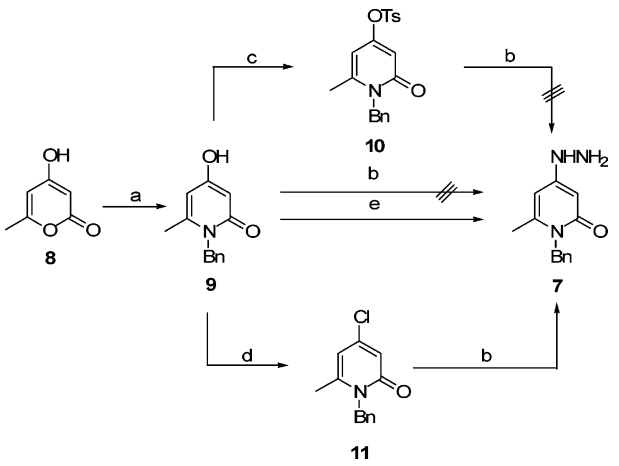

[a] Conditions: (a) $BnNH_2$, H_2O, Δ; (b) $NH_2NH_2 \cdot H_2O$, solvent, Δ; (c) *p*-TsCl, Py, rt; (d) $POCl_3$, 80 °C; (e) $NH_2NH_2 \cdot H_2O$, microwaves 250 W, 6 min.

Consequently, a different synthetic strategy was devised involving protection/deprotection of the 2-pyridone moiety. The retrosynthesis is briefly presented in Scheme 1. It was anticipated that alkylation of the benzyl-protected N2(9) analogue **6**, obtained by using *N*-benzyl-protected hydrazine **7** in the Fischer indole synthesis (Scheme 1), should proceed regioselectively to afford the N5(12)-alkylated derivatives **4** and **5**, respectively, after removal of the benzyl group.

The synthesis of hydrazine **7** starts from commercially available 4-hydroxy-6-methyl-2(1*H*)-pyran-2-one **8**. The reaction between compound **8** and an equimolar amount of benzylamine has been reported in the literature (Scheme 2).[22]

The formation of the 4-(benzylamino) derivative of the desired *N*-benzyl-4-hydroxy-2-pyridone **9** as a major side product in this reaction was noted; however, further experimental details and the yield of **9** were not reported.[22] In our hands, reaction of **8** with an equimolar amount of benzylamine in water afforded **9** in 56% yield.

Nucleophilic substitution of the hydroxy group in **9** was expected to proceed readily under the conditions analogous to the synthesis of the corresponding non-*N*-benzylated hydrazine.[23] Nevertheless, attempts to obtain hydrazine **7** directly from **9** (Scheme 2) by using an excess of the hydrazine monohydrate in boiling 2-ethoxyethanol or methanol yielded inseparable mixtures. Reaction of **9** with *p*-TsCl in pyridine afforded the tosylate **10** in quantitative yield. However, treatment of **10** with the hydrazine monohydrate in dry DMF failed to give **7**. Apparently, hydrazinolysis of **10** takes place instead of the nucleophilic substitution in the reaction with hydrazine monohydrate since the hydroxy derivative **9** and *p*-toluenesulfonylhydrazide were isolated in a couple of runs.

Finally, the hydrazine **7** could be prepared in a good yield from the chlorinated derivative **11** and hydrazine monohydrate in refluxing methanol (Scheme 2). Still this approach was frustrating owing to the low yield of **11**, probably due to acid-

(15) (a) Ducharme, Y.; Wuest, J. D. *J. Org. Chem.* **1988**, *53*, 5787−5789. (b) Zimmerman, S. C.; Duerr, B. F. *J. Org. Chem.* **1992**, *57*, 2215−2217. (c) Gallant, M.; Phan Viet Minh, T.; Wuest, J. D. *J. Am. Chem. Soc.* **1991**, *113*, 721−723. (d) Gallant, M.; Phan Viet Minh, T.; Wuest, J. D. *J. Org. Chem.* **1991**, *56*, 2284−2286. (e) Simard, M.; Su, D.; Wuest, J. D. *J. Am. Chem. Soc.* **1991**, *113*, 4696−4698. (f) Persico, F.; Wuest, J. D. *J. Org. Chem.* **1993**, *58*, 95−99. (g) Breeze, S. R.; Wang, S. *Inorg. Chem.* **1993**, *32*, 5981−5989. (h) Wang, X.; Simard, M.; Wuest, J. D. *J. Am. Chem. Soc.* **1994**, *116*, 12119−12120. (i) Boucher, E.; Simard, M.; Wuest, J. D. *J. Org. Chem.* **1995**, *60*, 1408−1412. (j) Munakata, M.; Wu, L. P.; Yamamoto, M.; Kuroda-Sowa, T.; Mackawa, M. *J. Am. Chem. Soc.* **1996**, *118*, 3117−3124. (k) Vaillantcourt, L.; Simard, M.; Wuest, J. D. *J. Org. Chem.* **1998**, *63*, 9746−9752. (l) Akazome, M.; Suzuki, S.; Shimizu, Y.; Henmi, K.; Ogura, K. *J. Org. Chem.* **2000**, *65*, 6917−6921. (m) Murguly, E.; McDonald, R.; Branda, N. R. *Org. Lett.* **2000**, *2*, 3169−3172. (n) Aakeroy, C. B.; Beatty, A. M.; Nieuwenhuyzen, M.; Zou, M. *Tetrahedron* **2000**, *56*, 6693−6699. (o) Plater, M. J.; Aiken, S.; Bourhill, G. *Tetrahedron Lett.* **2001**, *42*, 2225−2229. (p) Edwards, M. R.; Jones, W.; Motherwell, W. D. S. *Cryst. Eng.* **2002**, *5*, 25−36. (q) Du, Y.; Creighton, C. J.; Tounge, B. A.; Reitz, A. B. *Org. Lett.* **2004**, *6*, 309−312. (r) Olsezewska, T.; Gdaniec, M.; Połoński, T. *J. Org. Chem.* **2004**, *69*, 1248−1255. (s) Jónsson, S.; Solano Arribas, C.; Wendt, O. F.; Siegel, J. S.; Wärnmark, K. *Org. Biomol. Chem.* **2005**, *3*, 996−1001.
(16) Stončius, S.; Butkus, E.; Žilinskas, A.; Larsson, K.; Öhrström, L.; Berg, U.; Wärnmark, K. *J. Org. Chem.* **2004**, *69*, 5196−5203.
(17) (a) For a qualitative treatment, the PM3 level of calculations has been chosen. (b) *SPARTAN Pro*, version 1.0.5; Wavefunction, Inc.: 1840 Von Karman Avenue, Suite 370, Irvine, CA 92612.
(18) Mahadevan, I.; Rasmussen, M. *Tetrahedron* **1993**, *49*, 7337−7352.
(19) Comins, D. L.; Jianhua, G. *Tetrahedron Lett.* **1994**, *35*, 2819−2822.
(20) Guo, Z.-X.; Cammidge, A. N.; McKillop, A.; Horwell, D. C. *Tetrahedron Lett.* **1999**, *40*, 6999−7002.
(21) Bisagni, E.; Huang, N.-C. *Tetrahedron* **1986**, *42*, 2303−2309.
(22) Castillo, S.; Ouadahi, H.; Herault, V. *Bull. Soc. Chim. Fr.* **1982**, *2*, 257−261.
(23) Bisagni, E.; Ducrocq, C.; Civer, A. *Tetrahedron* **1976**, *32*, 1383−1390.

Scheme 3[a]

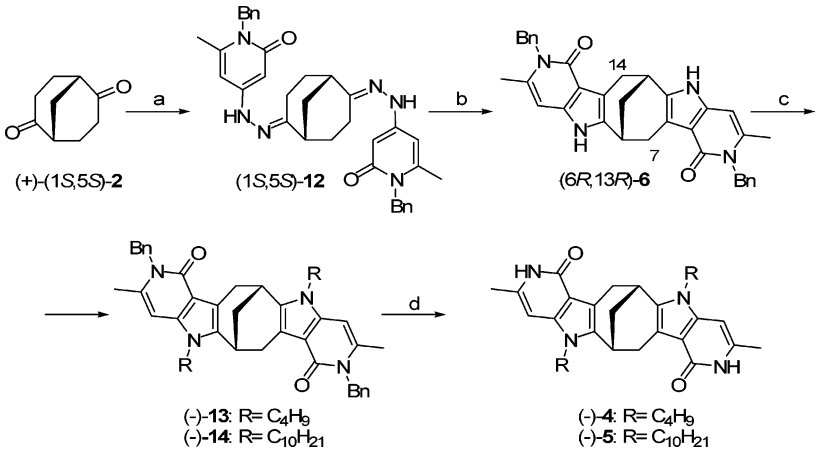

[a] Conditions: (a) **7**, MeOH, Δ; (b) Ph_2O, Δ; (c) DMF, NaH, RBr/KI or RI, rt; (d) Na, NH_3:THF.

catalyzed debenzylation in the reaction of **9** with neat $POCl_3$.[24] Attempts to use $SOCl_2$ or $POCl_3$ in combination with PCl_5 in the synthesis of **11** did not improve the yield.

It has been reported that nucleophilic substitution of the hydroxy group in the reaction of **9** with some amines is significantly facilitated by microwave irradiation.[25] In recent years, microwave irradiation has been used to enhance a great number of classical organic reactions leading to shorter reaction times and improved yields.[26] We attempted a direct solvent-free conversion of **9** to hydrazine **7** under microwave irradiation using an excess of hydrazine hydrate. Formation of **7** along with some side products was observed even at 250 W irradiation. The optimal ratio **9**:hydrazine hydrate was found to be 1:9, and optimal conditions were irradiation at 250 W for 6 min to afford **7** (57% yield) from **9** in a single step. The obtained hydrazine **7** was used further in the Fischer indole synthesis analogous to the synthesis of the parent compound **3** (Scheme 3).[16]

Treatment of hydrazine **7** with (+)-**2** in boiling methanol furnished bishydrazone (1*S*,5*S*)-**12** as a mixture of *E*,*E* and *E*,*Z*-isomers in high yield. The diketone (+)-**2** was obtained in enantiomerically pure form using enzymatic kinetic resolution of (±)-**2** mediated by Baker's yeast.[13] Although the enzymatic reduction of racemic bicyclo[3.3.1]nonane-2,6-dione is reported in the literature, the enantiomeric excess obtained is not high nor always reproducible, especially on a larger scale. We found that repeated fermentation with Baker's yeast for prolonged time afforded virtually the single enantiomer (+)-**2** (ee >99% GC). The racemic dione (±)-**2** was prepared from Meerwein's ester[27] by an improved procedure reported by Lightner.[28,29]

Subsequent thermal Fischer indole cyclization of (1*S*,5*S*)-**12** in boiling diphenyl ether afforded *N*-benzylated 2,9-diaza-6,13-methanocycloocta[1,2-b:5,6-b′]diindole, (6*R*,13*R*)-**6**. Both (6*R*,13*R*)-**6** and (1*S*,5*S*)-**12** were even less soluble compared to the corresponding nonbenzylated congeners.[16] Compound (6*R*,13*R*)-**6** could be dissolved only in mixtures of chloroform and TFA. Sixteen distinct resonance signals of carbon atoms in the ^{13}C NMR spectrum are in agreement with a C_2-symmetric structure of (6*R*,13*R*)-**6**. Interestingly, the ^1H NMR resonance signal corresponding to diastereotopic protons of the CH_2Ph groups appears as a pair of geminally coupled doublets, indicating hindered rotation around the N−CH_2 bonds in (6*R*,13*R*)-**6**. A relevant feature characteristic for Tröger's base analogues, namely, geminal coupling between H-7(14) *endo*- and *exo*-protons of benzylic-type methylene groups of the bicyclic skeleton, is also observed in the ^1H NMR spectrum of (6*R*,13*R*)-**6**. Detailed NMR analyses of the Tröger's base and some heterocyclic analogues[30] led to the assignment of the upfield signal to *endo*-protons and downfield signal to *exo*-protons of the benzylic methylene groups, though bis(acridine) analogues proved to be an exception to this rule. The chemical shift of the *exo*/*endo* protons has been shown to be influenced by the nature of the heterocyclic rings, the effect being more pronounced for the *endo*-protons, which are located inside the cavity and therefore very sensitive to the nature of the opposite ring. In the ^1H NMR spectrum of (6*R*,13*R*)-**6**, a doublet assigned to the H_{endo}-7(14) protons appears at δ 3.34 ppm, whereas a doublet of doublets at δ 3.16 ppm corresponds to H_{exo}-7(14) protons.

Alkylation of the dianion generated from (6*R*,13*R*)-**6** using NaH as the base in dry DMF at ambient temperature with 1-bromobutane/KI or 1-iododecane (or 1-bromodecane/KI) afforded the corresponding N5(12)-butyl and -decyl derivatives (−)-**13** and (−)-**14**, respectively (Scheme 3).

The final step in the synthesis of the target molecules (−)-**4** and (−)-**5** involved *N*-benzyl deprotection of the 2-pyridone moieties (Scheme 3). Attempts to cleave the benzyl groups in (−)-**14** by catalytic hydrogenation (20% $Pd(OH)_2/C$)[31] at room

(24) Kappe, T.; Ajili, S.; Stadlbauer, W. *J. Heterocycl. Chem*. **1988**, *25*, 463−468.
(25) Heber, D.; Stoyanov, E. V. *Synlett* **1999**, *11*, 1747−1748.
(26) Lindström, P.; Tierney, J.; Wathey, B.; Westman, J. *Tetrahedron* **2001**, *57*, 9225−9283.
(27) Meerwein, H.; Schürmann, W. *Liebigs Ann*. **1913**, *398*, 196.
(28) Lightner, D. A.; Chang, T. C.; Hefelfinger, D. T.; Jackman, D. E.; Wijekoon, W. M.; Givens, J. W., III. *J. Am. Chem. Soc*. **1985**, *107*, 7499−7508.
(29) For other examples of the synthesis of Meerwein's ester and bicyclo[3.3.1]-nonane-2,6-dione, see: (a) Stetter, H.; Held, H.; Schulte-Oestrich, A. *Chem. Ber*. **1962**, *95*, 1687−1691. (b) Föhlisch, B.; Dukek, U.; Graessle, I.; Novotny, B.; Schupp, E.; Schwaiger, G. *Liebigs Ann*. **1973**, 1839. (c) Shaefer, J. P.; Hong, L. M. *J. Org. Chem*. **1968**, *33*, 2655−2659. (d) Quast, H.; Witzel, M. *Liebigs Ann*. **1993**, 699−700. (e) Mislin, G.; Miesch, M. *Eur. J. Org. Chem*. **2001**, 1753−1759.
(30) (a) Demeunynck, M.; Tatibouët, A. Recent Developments in Tröger's Base Chemistry. In *Progress in Heterocyclic Chemistry*; Gribble, G. W., Gilchrist, T. L., Eds.; Pergamon: Oxford, 1999; Vol. 11, pp 1−20 and references therein. (b) Abonia, R.; Albornoz, A.; Larrahondo, H.; Quiroga, J.; Insuasty, B.; Insuasty, H.; Hormaza, A.; Sanchez, A.; Nogueras, M. *J. Chem. Soc., Perkin Trans. 1* **2002**, 1588−1591.
(31) Tahri, A.; Buysens, K. J.; Van der Eycken, E. V.; Vandenberghe, D. M.; Hoornaert, G. J. *Tetrahedron* **1998**, *54*, 13211−13226.

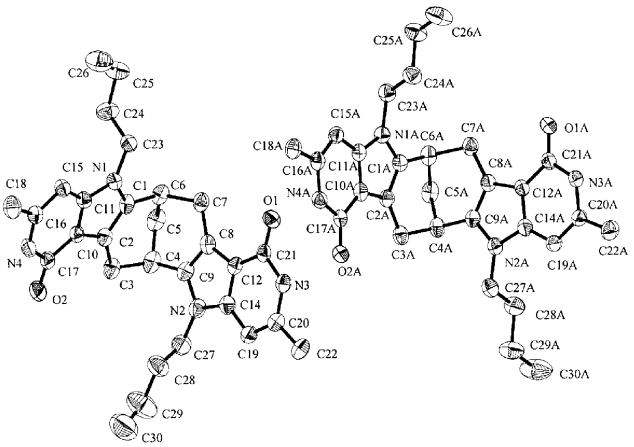

Figure 3. Crystal structure of (−)-**4**·CH_3CN. DIAMOND view of the two molecules A and B constituting the asymmetric unit cell. The CH_3CN molecules and hydrogen atoms are omitted.

temperature failed. After stirring for 9 days in acetic acid, the formation of a mixture of products was observed together with a substantial amount of the starting material still present in the reaction mixture. Compound (−)-**14** remained unaffected after stirring or heating under reflux in TFA[32] or after treatment with sodium in liquid ammonia[33] at −78 °C for 1.5 h. Nevertheless, traces of (−)-**5** were obtained after 6 h of reaction in a mixture of NH_3 and THF (∼10:1) at −78 °C.[34] The yield of (−)-**5** could be improved by increasing temperature and the amount of THF in the reaction mixture: performing the reduction of (−)-**14** in a mixture of NH_3 and THF (∼3:1) at −45 °C furnished (−)-**5** in 59% yield. Addition of (−)-**14** to a preformed solution of Na in a mixture of NH_3 and THF (∼1:1) led to further improvement of yield (83%). Meanwhile, deprotection of (−)-**13** in a mixture of NH_3 and THF (∼3:1) at −45 °C proceeded smoothly to give (−)-(6*R*,13*R*)-**4** in excellent yields (89−91%).

^1H and ^{13}C NMR spectral data are in agreement with C_2-symmetric structures of (−)-**4**, (−)-**5**, (−)-**13**, and (−)-**14**. Rotation of the alkyl chains around C−N5(12) bonds in those compounds is notably hindered since the diastereotopic protons of methylene groups are geminally coupled and the corresponding resonance signals appear as a pair of double triplets in the ^1H NMR spectra. The obtained compounds (−)-**5** and (−)-**4** were soluble in chlorinated solvents as expected.

Association in the Solid State. Single crystals of (−)-**4** suitable for X-ray diffraction analysis were obtained by slow evaporation of a solution of (−)-**4** in acetonitrile. X-ray structure analysis revealed two crystallographically independent molecules of (−)-**4**, A and B, together with two molecules of acetonitrile in the unit cell. DIAMOND representations of the two molecules of (−)-**4**·CH_3CN, differing by the conformation of *n*-butyl chains, in the asymmetric units are shown in Figure 3.

Association of (−)-**4** in the solid state failed to give the anticipated helical tubular structure based on the centrosymmetric hydrogen bonding between self-complementary 2-pyridone AD−DA motifs. Instead, the crystal structure of (−)-**4** reveals the formation of infinite supramolecular hydrogen-bonded networks in which one molecule of (−)-**4** is hydrogen bonded to four neighboring molecules via four distinct A−D hydrogen bonds between C═O and N−H of different 2-pyridone moieties in different molecules of (−)-**4** (Figure 4).

More specifically, the two cavity molecules of (−)-**4** are interlinked by a single A−D hydrogen bond between the C═O group in the 2-pyridone moiety in one molecule of (−)-**4** and the N−H group in the 2-pyridone moiety of another molecule of (−)-**4** (Table 1). The remaining N−H and C═O functionalities in the two cavity molecules participate in the propagation of the hydrogen-bonded chain by association with the next two adjacent cavity molecules. The hydrogen-bonded network, extending in the two directions along crystallographic *a* and *c* axes, is shown in Figure 4a.

Interestingly, the two types of hydrogen-bonded A−D chains, ···O═C−N−H···O═C−N−H···O═C−N−H···, involved in the formation of hydrogen-bonded networks are indeed helical (Figure 4b). Both chains running along the crystallographic *a* axis comprise right-handed (P) helices. The corresponding dihedral angles (C21A)−N3A−(C17)−N4, (C17)−N4−(C21A)−N3A, (C17A)−N4A−(C21)−N3, and (C21)−N3−(C17A)−N4A for the two types of chains are found to be 81.46(48), 89.39(43), 58.39(48), and 71.44(41)°, respectively. This indicates arrangement of 2-pyridone motifs of the neighboring cavity molecules in the aggregate closer to perpendicular, dissimilar to the expected centrosymmetric hydrogen-bonded dimer of 2-pyridone motifs with a dihedral angle equal to zero.

In addition to hydrogen bonding, the packing of (−)-**4** is assisted by heteroaryl face−C−H (aliphatic) interactions leading to columns of stacked shape-complementary cavities. The single-stacked column running along the crystallographic *a* axis consists of crystallographically symmetry-equivalent molecules, that is, only A or B. In the so formed columns, the apex of one molecule is accommodated in the cavity of another with the apex-to-apex C···C distances practically identical for both fragments, namely, 5.371(6) and 5.371(8) Å for A and B, respectively. Columns are packed along the *c* axis in repeated A···B···A order and are interconnected by A−D hydrogen bonds between C═O and N−H of 2-pyridone motifs belonging to A and neighboring B. The side view of the three stacks is shown in Figure 4a.

Cavity molecules of (−)-**4** are packed in columns and interconnected by multiple hydrogen bonds, forming planar layers extending along crystallographic *a* and *c* axes. Neighboring layers are packed in a parallel fashion, but differ by the opposite arrangement of the cavity apexes packed in columns. The *n*-butyl chains emerge from both sides of the layers, forming a hydrophobic coating. The top view of the two parallel layers is shown in Figure 5.

The arrangement of the *n*-butyl chains in the interlayer space forms voids along the crystallographic *a* axis, which are filled with solvent molecules. The view of the four channels is shown in Figure 5. The CH_3CN molecules in the channels are arranged in a parallel fashion with an intermolecular distance coinciding with the apex-to-apex distance (5.371 Å) between cavity molecules in columnar stacks.

Similarly to the crystal structure of (±)-**3**,[16] heteroaryl face−C−H (aliphatic) interactions contribute significantly to the lattice packing of (−)-**4**. Analogous apex-to-apex packing of shape-

(32) Padwa, A.; Heidelbaugh, T. M.; Kuethe, J. T. *J. Org. Chem.* **2000**, *65*, 2368−2378.
(33) Meade, E. A.; Beauchamp, L. M. *J. Heterocycl. Chem.* **1996**, *33*, 303−308.
(34) Merz, A.; Meyer, T. *Synthesis* **1999**, 94−99.

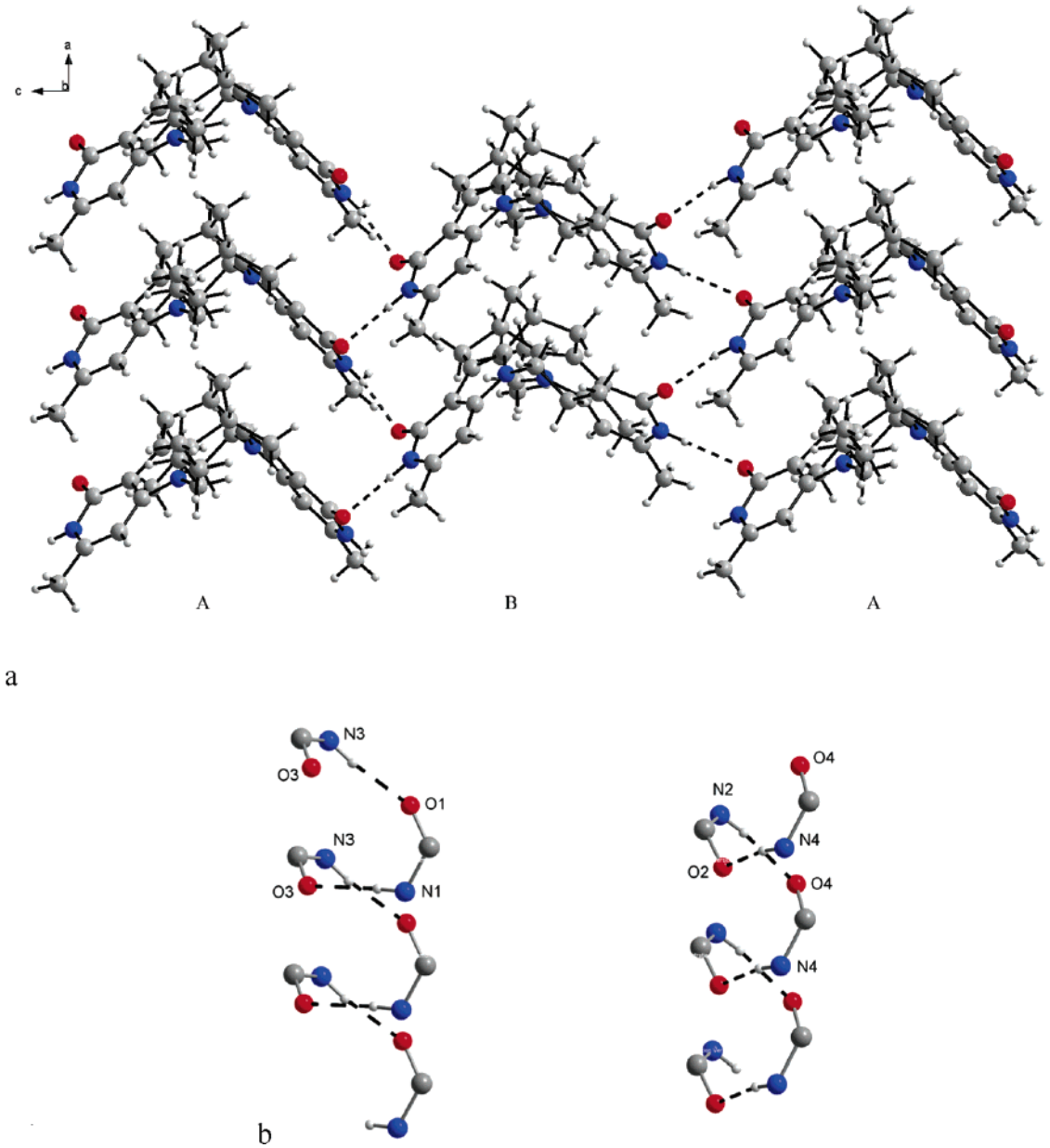

Figure 4. Hydrogen-bond network in the crystal structure of (−)-**4**·CH_3CN. (a) Side view of hydrogen-bonded network and columnar stacks. (b) Two helical A−D hydrogen-bonded chains, ···O═C−N−H···O═C−N−H···. See Figure 3 for the numbering of the atoms.

Table 1. Geometry of the Intermolecular Hydrogen Bonds in (−)-**4**·CH_3CN

donor[a]	hydrogen	acceptor[a]	D···A (Å)	∠DHA (deg)[b]
N3A	H(N3A)	O2	2.819(4)	162.73(31)
N4A	H(N4A)	O1	2.789(4)	169.52(30)
N4	H(N4)	O1A	2.955(3)	175.73(31)
N3	H(N3)	O2A	2.899(4)	170.36(30)

[a] See Figures 3 and 4 for numbering of the atoms. [b] The D−H in the 2-pyridone plane.

complementary cavities leading to the columns of stacked molecules has been noted for carbocyclic cavities.[35]

The hydrogen-bonding feature incorporated in the carbocyclic cavity molecule of (−)-**4** is apparently insufficiently robust to yield the anticipated helical tubular supramolecular structure based on the 2-pyridone motif, at least in the solid state. A similar result was reported recently for 6-methyl-2-pyridone, showing that indeed hydrogen-bonded A−D chains, ···O═C−N−H···O═C−N−, are involved in the intermolecular self-aggregation of 6-methyl-2-pyridone in the solid state.[36] In contrast, for the parent compound, (±)-**3**, crystallized from DMF, one of the two self-complementary 2-pyridinone hydrogen-bonding AD−DA motifs, is involved in self-aggregation.[16]

Association in Solution. NMR Titrations. The aggregation behavior of the more soluble homologue (−)-**5** (Figure 1) was investigated by using the concentration dependence of the ^1H NMR chemical shifts. The shift of the NH proton resonance of the 2-pyridone moieties of (−)-**5** in $CDCl_3$ and CD_2Cl_2 showed a remarkable concentration dependence (Figure 6), clearly

(35) Field, J. D.; Turner, P.; Harding, M. M.; Hatzikominos, T.; Kim, L.; *New J. Chem.* **2002**, *26*, 720−725.

(36) Nichol, G. S.; Clegg, W. *Acta Crystallogr.* **2005**, *C61*, o383−o385.

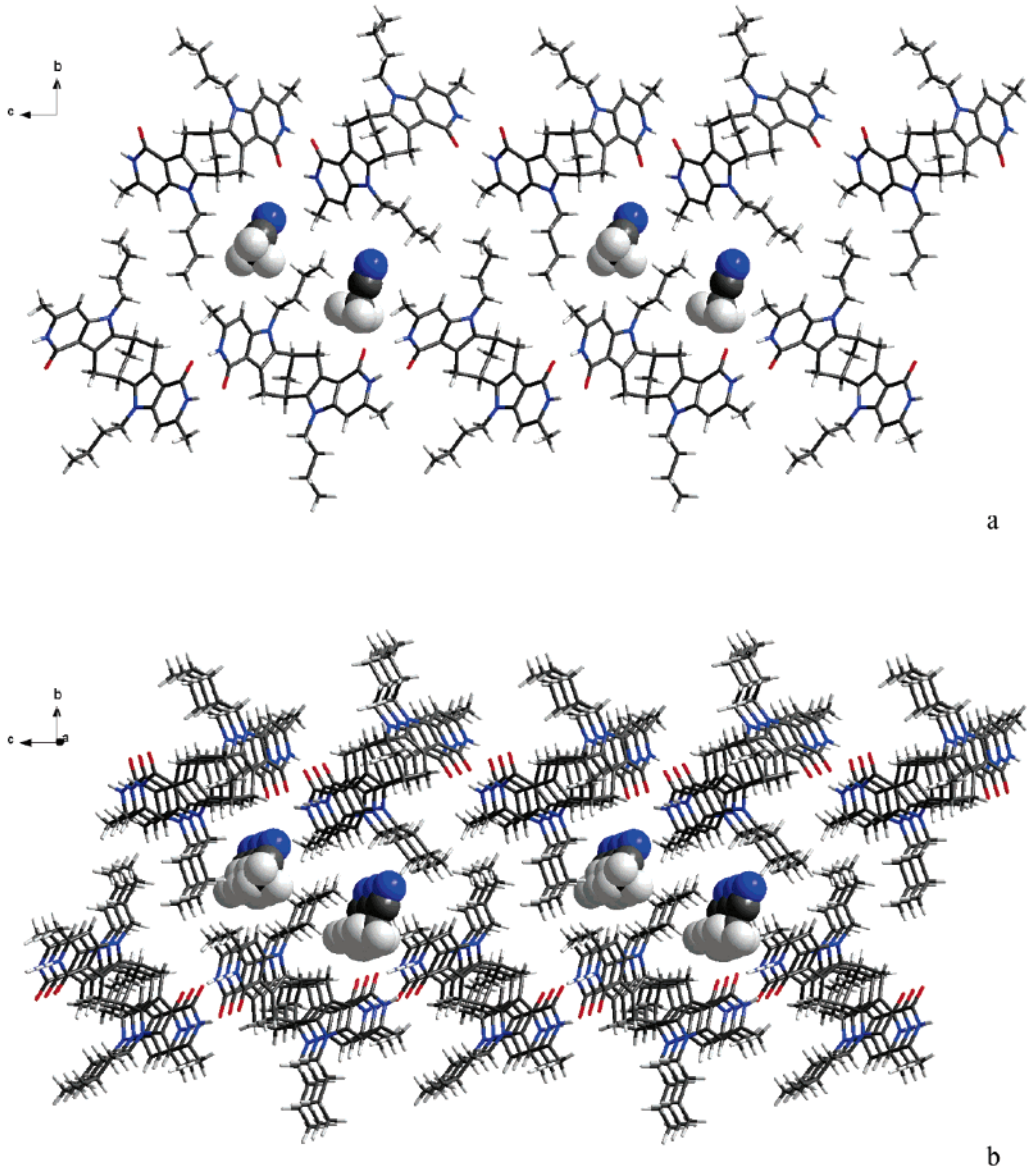

Figure 5. Crystal structure of (−)-**4**·CH_3CN. The top view of the two parallel layers, showing the four channels with solvent molecules (a) and the three-dimensional extension of the channels (b).

indicating that intermolecular association via its self-complementary 2-pyridone motifs occurs.

NMR titration is widely used to observe and quantify the association processes by estimating the association constants of supramolecular aggregates.[37] For an associate in fast exchange on the NMR time scale, the observed chemical shift of a particular proton is the weighted average of the chemical shifts in the native (nonexchanging) environments, that is, monomer and associates in this particular case.

Assuming the formation of higher than dimeric aggregates, NMR dilution titration data were analyzed by using the isodesmic model of indefinite association ($K_1 = K_2 = ... = K_n = K_E$) for the formation of supramolecular polymers (linear aggregates).[38] In this model, it is assumed that the free energy, and thus the association constant K_E, for the successive addition of each monomer to an aggregate is identical (equal K model). The chemical shift δ for each of the studied proton resonances then depends on the total concentration, c_t, of the monomer and the association constant, K_E, according to eq 1[38,39]

$$\delta = \delta_m + (\delta_a - \delta_m)\left(1 + \frac{1 - \sqrt{4K_E c_t + 1}}{2K_E c_t}\right) \qquad (1)$$

where δ_m and δ_a are the chemical shift of the studied proton resonance in the monomer and the average shift in the aggregates, respectively. By measuring the observed chemical shift(s) of the observed proton resonance(s), δ_{obs}, at different values of c_t, a data set is obtained. By using a nonlinear curve fitting procedure in which the parameters δ_m, δ_a, and K_E in eq 1 are estimated to give the best fit of $\delta = f(c_t)$ to the observed data set (δ_{obs}, c_t), an estimate of K_E can be obtained.

We also wanted to estimate the change in enthalpy and entropy for the association of the 2-pyridone binding site in

(37) Fielding, L. *Tetrahedron* **2000**, *56*, 6151−6170.
(38) Martin, R. B. *Chem. Rev.* **1996**, *96*, 3044−3064.
(39) Tobe, Y.; Utsumi, N.; Kawabata, K.; Nagano, A.; Adachi, K.; Araki, S.; Sonoda, M.; Hirose, K.; Naemura, K. *J. Am. Chem. Soc.* **2002**, *124*, 5350−5364.

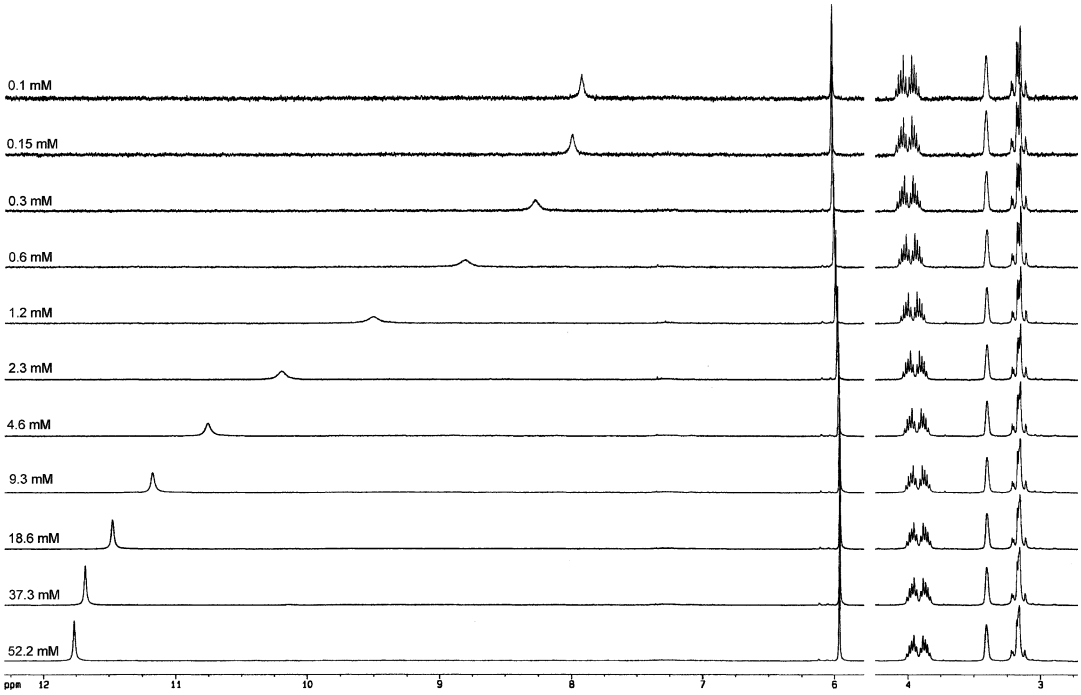

Figure 6. Parts of the ^{1}H NMR spectra (400 MHz, CD_2Cl_2, 299 K) of (−)-**5** at different concentrations.

the monomer to another such site in an aggregate (polymerization) or in another monomer (dimerization) using the same model. Usually, estimates of the association constant K_E at different temperatures, determined, for example, by the methodology described above, are used in a linear curve fitting procedure of the van't Hoff's eq 2 to give estimates of ΔH^0 and ΔS^0.

$$\ln K_E = -\frac{\Delta H^0}{R}\frac{1}{T} + \frac{\Delta S^0}{R} \qquad (2)$$

However, instead of estimating K_E values at each investigated temperature using the procedure above, using eq 1, a globally better fit of δ to δ_{obs} can be obtained by a nonlinear curve fitting procedure, where the parameters δ_m, δ_a, ΔH^0, and ΔS^0 in eq 3, obtained by combining eqs 1 and 2, are estimated to give the best fit of $\delta = f(c_t,T)$ to the observed data set (δ_{obs}, c_t, T) (see Supporting Information). In this way, estimation of ΔH^0, ΔS^0, and thus K_E at different temperatures is obtained with higher accuracy.

$$\delta = \delta_m + (\delta_a - \delta_m)\left(1 + \frac{1 - \sqrt{4c_t \exp\left(-\frac{\Delta H^0}{R}\frac{1}{T} + \frac{\Delta S^0}{R}\right) + 1}}{2c_t \exp\left(-\frac{\Delta H^0}{R}\frac{1}{T} + \frac{\Delta S^0}{R}\right)}\right) \qquad (3)$$

A single set of signals corresponding to the NH proton resonance of (−)-**5** was observed throughout the concentration range with some sharpening of the signals upon dilution. In $CDCl_3$, 10 different concentrations (79.0−0.667 mM) at five different temperatures (258−311 K) were investigated giving in total 50 data points (Figure 7 and Supporting Information Table S1).

By using the nonlinear curve fitting procedure of the data points in Figure 7 to the isodesmic model of indefinite

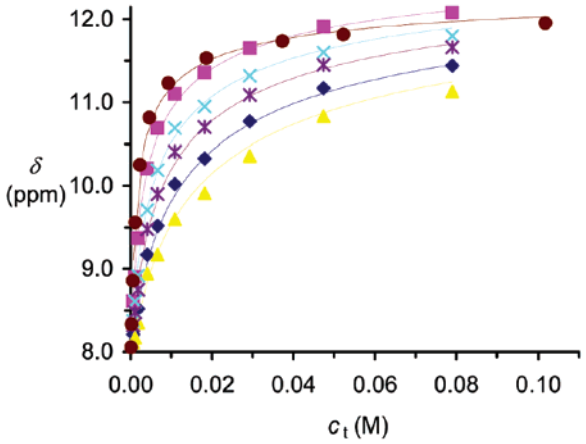

Figure 7. Observed chemical shifts of the NH proton resonance of (−)-**5** in $CDCl_3$ and CD_2Cl_2, respectively, at different concentrations and temperatures. The solid lines represent the best fit of the observed data to the isodesmic model of indefinite association as expressed by eq 3. In $CDCl_3$: 258 K (■), 272 K (×), 284 K (∗), 299 K (◆), 311 K (▲). In CD_2Cl_2: 299 K (●).

association as expressed in eq 3, ΔH^0 and ΔS^0 were estimated to −20.3 ± 1.2 kJ mol^{-1} and −29.1 ± 4.2 J mol^{-1} K, respectively, in a 95% confidence interval. The chemical shifts of the NH proton resonance of free and associated (−)-**5**, δ_m and δ_a, were estimated to be 7.75 ± 0.10 and 12.91 ± 0.12 ppm, respectively, in a 95% confidence interval. The estimated value of ΔH^0 is slightly lower than the corresponding experimental value obtained for the dimerization of 2-pyridone itself in $CHCl_3$ (−24.7 kJ mol^{-1}),[40] corresponding to twice the heat of formation of a single N−H···O═C hydrogen bond in $CHCl_3$.[41] This slightly lower value of ΔH^0 can be explained by some steric interaction between the two interacting 2-pyridone

(40) (a) Hammes, G. G.; Park, A. C. J. *Am. Chem. Soc.* **1969**, *91*, 956−961. (b) Hammes, G. G.; Spivey, H. O. *J. Am. Chem. Soc.* **1966**, *88*, 1621−1625.
(41) Pimental, G. C.; McClellan, A. L. *The Hydrogen Bond*; W. H. Freeman and Co: San Francisco, 1960.

Table 2. Estimation of the Association Constant K_E for the Indefinite Association of (−)-**5** in $CDCl_3$ According to the Isodesmic (equal *K*) Model of Indefinite Association[a]

T (K)	$K_E \times 10^{-3}$ (M^{-1})
258	0.38 (0.33, 0.44)[b]
272	0.24 (0.20, 0.27)[b]
284	0.162 (0.141, 0.183)[b]
299	0.105 (0.0921, 0.119)[b]
311	0.0765 (0.0670, 0.0873)[b]

[a] The value of K_E at each of the investigated temperatures *T* is obtained from the ΔH^0 and ΔS^0 values using eq 2. [b] At 95% confidence interval of $K_E \times 10^{-3}$. Obtained from exponentiation of the result of an error propagation analysis[42] using the variance and covariance of ΔH^0 and ΔS^0 and eq 2 for the estimate of the variance of ln K_E.

units due to the presence of the methyl group in the 3 and 10 positions in (−)-**5**. Nevertheless, the similarity of the ΔH^0 values indicates that the 2-pyridone motif of (−)-**5** is involved in self-complementary aggregation. Thus, since (−)-**5** is enantiomerically pure, the aggregate must be of tubular helical structure of the type depicted in Figure 2. The value of ΔS^0 for (−)-**5** is higher than the corresponding experimental value obtained for the dimerization of 2-pyridone itself in $CHCl_3$ (−42.7 J mol^{-1} K).[40] This can be explained by the fact that the somewhat looser self-association of (−)-**5** compared to that of 2-pyridone, as seen by the corresponding ΔH^0 values, allows for a bit more conformational binding freedom in the former case than in the latter. By using eq 2, K_E for each investigated temperature could now be computed from the estimated values of ΔH^0 and ΔS^0 (see Table 2).

As anticipated, (−)-**5** associates much more strongly in CD_2Cl_2, which is less C−H acidic compared to $CDCl_3$, and thus less competitive for hydrogen bonding with the carbonyl of the 2-pyridone motif. The upfield shift of the NH proton resonance from δ 11.9 to 7.93 was observed as the concentration decreased from 102 to 0.102 mM (Figure 7). Using the nonlinear curve fitting procedure of the isodesmic model of indefinite aggregation as eq 1 to the experimental data points (see Supporting Information, Table S2), 12 in total, gave the association constant K_E for the aggregation of (−)-**5** in CD_2Cl_2 at 299 K as estimated to be $(1.14 \pm 0.32) \times 10^3$ M^{-1} in a 95% confidence interval. The chemical shifts of the NH proton resonance of free and associated (−)-**5**, δ_m and δ_a, were calculated to be 7.34 ± 0.24 and 12.44 ± 0.16 ppm, respectively, in a 95% confidence interval.

To rule out the involvement of another possible type of aggregation, $\pi-\pi$ stacking, and thus strengthening the suggested proposal about helical tubular mode of aggregation, a closer inspection of the different ^{1}H NMR spectra obtained from the dilution titrations of (−)-**5** was undertaken. Only a small chemical shift change of the resonance signals corresponding to the heteroaromatic methine and C3(10)−CH_3 group protons (see Figure 1 for numbering of atoms) was observed (Figure 8). The chemical shifts of these protons should be significantly affected in the case of self-association due to $\pi-\pi$ stacking.[39,43] Thus, such $\pi-\pi$ interactions are not likely to occur, at least not in the concentration range investigated. Moreover, both resonance signals of the heteroaromatic methine and CH_3 protons were slightly shifted upfield, by $\Delta\delta$ 0.03 and 0.07 ppm,

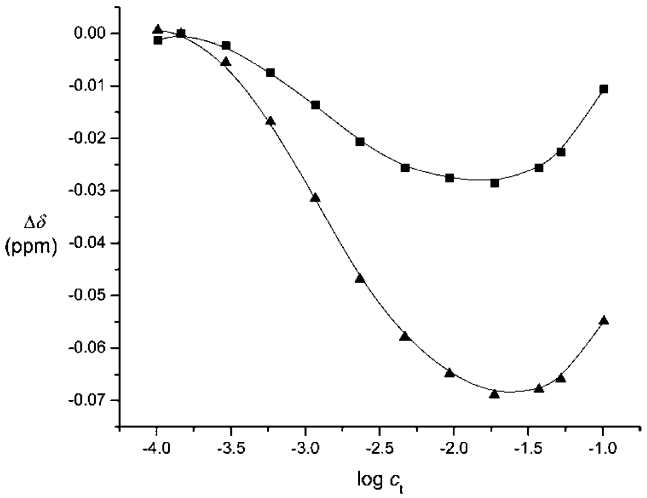

Figure 8. Concentration dependence of ^{1}H NMR chemical shifts of (−)-**5** in the concentration range of 102−0.102 mM for heteroaromatic methine (■) and C3(10)−CH_3 (▲) proton resonances in CD_2Cl_2 at 299 K. The lines are inserted trend lines.

respectively, as the concentration of (−)-**5** increased from 0.102 to 18.7 mM. It is likely that protons of the methyl group are affected intermolecularly by the shielding of the carbonyl group of the next associated molecule in the chain (cf. Figure 2), again confirming the suggested mode of aggregation involving the 2-pyridone hydrogen-bonding motif. Interestingly, 18.7 mM corresponds to an average degree of polymerization, DP = 5 (vide infra), meaning that, at this concentration, the presumed helix has completed one overlapping turn. Above 18.7 mM concentration, a downfield shift is observed, which probably can be attributed to the competing shielding/deshielding effects due to the interactions between the different turns, as the size of the helical aggregate increases.

VPO Measurements. It is important to rule out the possibility that the estimated association constants do not merely represent a dimerization model, as expressed by K_2. The isodesmic model for indefinite association, as expressed by K_E, cannot be distinguished from the dimerization model by NMR dilution titrations as can be seen by comparing eq 1 and the one for dimerization.[38,44] An independent method was needed to differentiate between the two cases.

The self-aggregation of solutes is frequently analyzed on the basis of the molal osmotic coefficient, Φ, determined by vapor pressure osmometry (VPO).[38] The fact that VPO measures colligative properties, such as actual number of moles in solution, makes it possible to distinguish dimerization from aggregation of a higher order. For the VPO measurements, the method of Ts'o and Chan was followed[45] (see Supporting Information) using nonlinear curve fitting. The ratio Φ/γ, where γ is the activity factor, was determined experimentally at 313 K for seven different true molal concentrations (activities) of monomer (−)-**5** in $CHCl_3$, m_1, obtained after correction of the observed molality by γ (Figure 9).

The data obtained (Figure 9) were fitted to the isodesmic model of indefinite association (equal *K* model), where $K_1 = K_2 = ... = K_n = K_E$ and $K_{n+1} = 0$. This model relates Φ/γ, m_1, the number of monomers in the largest aggregate (*n*) and K_E,

(42) Cameron, J. M. In *Encyclopedia of Statistical Sciences*; Kotz, S., Johnson, N. L., Eds.; Wiley: New York, 1982; p 549.
(43) Zhao, D.; Moore, J. S. *J. Org. Chem.* **2002**, *67*, 3548−3554.
(44) Horman, I.; Dreux, B. *Helv. Chim. Acta* **1984**, *67*, 754−764.
(45) Ts'o, P. O. P.; Chan, S. I. *J. Am. Chem. Soc.* **1964**, *86*, 4176−4181.

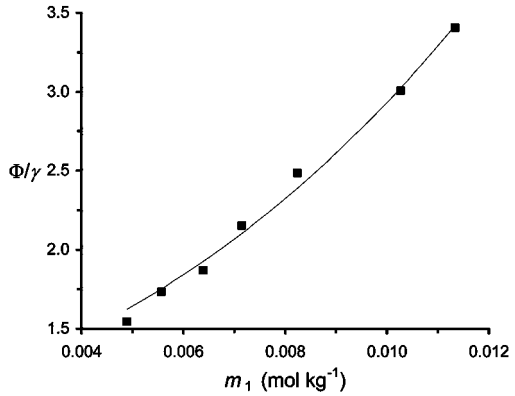

Figure 9. Observed ratio between the osmotic and activity coefficient, Φ/γ, at different true molal concentrations (activities) m_1 of (−)-**5** in $CHCl_3$ at 313 K. The solid line represents the best fit of the observed data to the isodesmic model of indefinite association (equal *K* model, eq 4).

according to eq 4.[45]

$$\frac{\Phi}{\gamma} = \frac{1 - (K_E m_1)^n}{1 - K_E m_1} \tag{4}$$

By using a nonlinear curve fitting procedure, K_E was estimated to be 120 ± 6 $M^{-1}$and n = 3.7 ± 0.3 in $CHCl_3$ at 313 K. The value of K_E obtained by VPO is in good agreement with the value obtained from the NMR dilution titrations at 311 K, 77 M^{-1}, keeping in mind the difference in temperature and the fact that VPO measurements in general give larger values of the association constant than NMR dilution titrations when the extent of aggregation is small.[39] More important, the VPO indicates that $n > 2$, thus refuting a dimer model, and thereby supporting the Equal *K* model in the NMR dilution titrations above.

The Degree of Polymerization. Refuting the dimerization model enables calculation of the average number of monomers in the associate (polymer) obtained by self-association of (−)-**5** (the degree of polymerization, DP) from the NMR dilution titrations. For the isodesmic model of self-aggregation, DP is calculated using eq 5, where c_m is the molar concentration of free monomer, obtained from the total molar concentration of monomer, (−)-**5** in solution (free and associated), c_t, eq 6.[46,38]

$$\mathrm{DP} = \frac{1}{1 - K_E c_m} \tag{5}$$

$$c_t = \sum_{i=1}^{\infty} i c_i = \sum_{i=1}^{\infty} i K_E^{-1} (K_E c_m)^i = \frac{c_m}{(1 - K_E c_m)^2} \quad \text{for } K_E c_m < 1 \tag{6}$$

The resulting curves showing DP as a function of the total molar concentration of (−)-**5**, c_t, in $CDCl_3$ and CD_2Cl_2, respectively, and at various temperatures are shown in Figure 10. As expected, the average size of the aggregate increases with decreasing temperature and with a less protic solvent (CD_2Cl_2).

We can conclude from the values of DP obtained from NMR dilution titrations and from the values of *n* obtained from the VPO measurements that (−)-**5** forms aggregates containing only a few monomers in $CDCl_3/CHCl_3$ at 299 K. However, in CD_2Cl_2, at 299 K, the aggregates contain up to 11 units of (−)-**5** on an average.

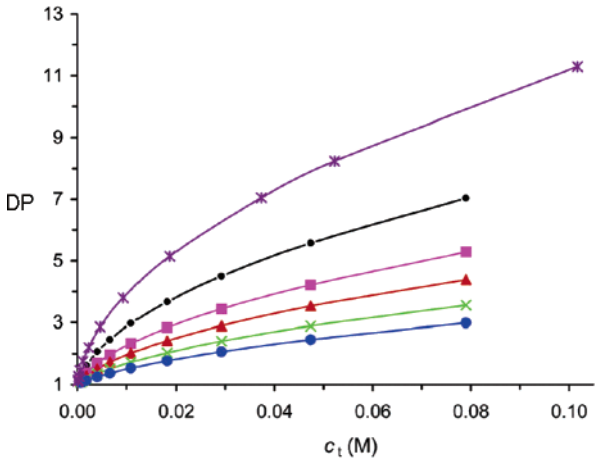

Figure 10. The average degree of polymerization, DP, as a function of the total molar concentration of (−)-**5**, c_t. In $CDCl_3$: 258 K (●), 272 K (■), 284 K (▲), 299 K (×), 311 K (●). In CD_2Cl_2: 299 K (∗).

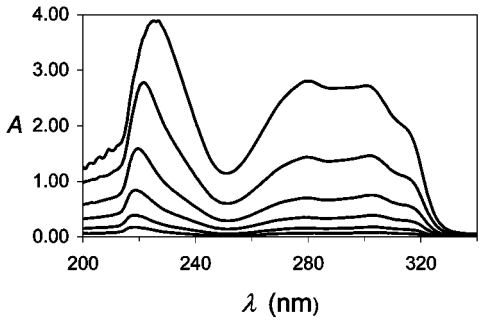

Figure 11. Electronic spectra of (−)-**5** in CH_2Cl_2 at concentrations 1.6, 0.80, 0.40, 0.20, 0.10, and 0.050 mM.

Electronic Spectroscopy. Electronic spectroscopy is well established to study aggregation. In our case, this method can be used to rule out $\pi-\pi$ stacking as a mode of aggregation for (−)-**5**. It is expected that direct electronic interactions between chromophores would cause spectral changes and, in most cases, a hypsochromic shift.[47] More precisely, in our case, a nonlinear behavior in the change of absorbance of (−)-**5** with concentration would indicate the presence of $\pi-\pi$ stacking. For the UV dilution titrations, a set of solutions in dry CH_2Cl_2 was prepared by dilution of the initial stock solution of (−)-**5** at 3.3 mM. Concentrations larger than 1.6 mM could not be used due to high absorbance in a 0.1 cm cell. Each solution in the set was a concentration 2-fold lower than the previous one. According to Figure 10 at 1.6 mM in CH_2Cl_2 at 299 K, the average number of monomers in the aggregates of (−)-**5** is two, and at 0.05 mM, only monomeric (−)-**5** exists based on the NMR titrations. Spectra from the UV titrations are presented in Figure 11. The absence of isosbestic points and the fact that the general appearance of the spectra does not change with concentration indicate that the monomers do not interact with each other's chromophores when forming aggregates, thus suggesting the absence of $\pi-\pi$ stacking in the concentration range studied. Furthermore, the spectra are similar to the ones for the di-*N*-benzyl-protected derivative (−)-**14** (see Supporting Information,

(46) Zhao, D.; Moore, J. S. *Org. Biomol. Chem.* **2003**, *1*, 3471−3491.

(47) See, for example: Diederich, F. *Cyclophanes*; Stoddart, J. F., Ed.; The Royal Society of Chemistry: Cambridge, 1991; pp 19−21.

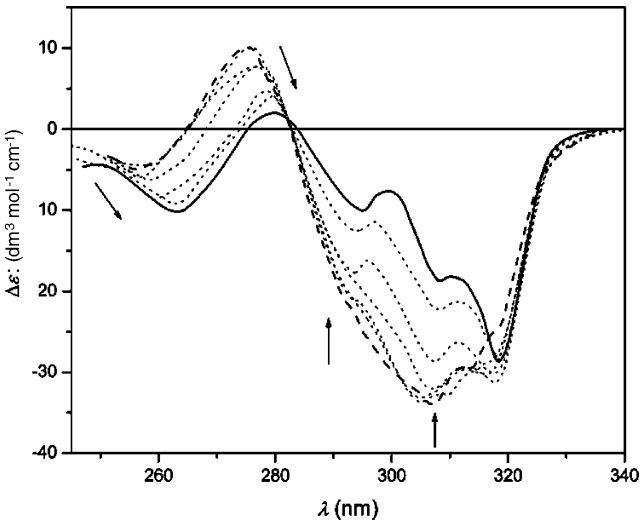

Figure 12. CD spectra of (−)-**5** in CH_2Cl_2 at concentrations from 3.3 mM (—) to 0.05 mM (- - -), each concentration is half of the previous higher one. Arrows indicate changes as concentration increases.

Figure S3), meaning that the absence of hydrogen bonding does not significantly change the electronic spectra.

Plots of the absorbance versus concentration for the three strongest absorptions in the electronic spectrum of (−)-**5** follow Lambert−Beer's law within the experimental errors (see Supporting Information, Figure S4). This result rules out the involvement of $\pi-\pi$ stacking in the concentration range investigated (see above). Basically, the same structure of the plot for the di-*N*-benzyl-protected derivative (−)-**14** is observed, excluding $\pi-\pi$ stacking as a mode of aggregation also for this compound (see Supporting Information, Figure S5).

Circular Dichroism (CD) Spectroscopy. CD spectroscopy has been shown to be an appropriate method to characterize optically active molecules containing elements of helicity.[48] The overall shape and intensity of the CD spectra of (−)-**5** in nonpolar solvents were anticipated to be dependent on concentration due to self-association. The CD spectra at various concentrations of the most soluble derivative containing the 2-pyridone motifs, compound (−)-**5**, were recorded in CH_2Cl_2 in which the self-association is more pronounced as evidenced by ^{1}H NMR spectroscopy. The CD spectra of (−)-**5** in the concentration range from 3.3 to 0.05 mM in CH_2Cl_2 (seven measurements) are presented in Figure 12. According to Figure 10 at 3.3 mM, the average aggregation of (−)-**5** is between 2 and 3, and at 0.05 mM, only monomeric (−)-**5** exists.

Obviously, the variations of $\Delta\epsilon$ in the CD spectra with different concentrations originate from the self-association of (−)-**5** via hydrogen bonding, as no changes were observed in the CD spectra of the *N*-benzylated congener, (−)-**14**, in the concentration range from 0.5 to 0.032 mM. In fact, upon plotting the change in $\Delta\epsilon$ for the Cotton effects in Figure 12 versus concentration at two arbitrary wavelengths, 265 and 275 nm, respectively, a rather strong concentration dependence is observed (see Supporting Information, Figure S6). Following the change in $\Delta\epsilon$ with concentration has been an appropriate method to evidence enantiospecific helical folding of achiral oligomers upon addition of suitable chiral guests[49] or amplification of chirality in mixed helical architectures composed of achiral and chiral monomers.[50] Herein, although the value of $\Delta\epsilon$ for (−)-**5** changes strongly upon aggregation, we cannot conclude from this observation whether this effect is caused by the alignments of chromophores of (−)-**5** in a helical pattern or whether the observed phenomenon is merely a demonstration of self-aggregation. To acquire a conclusive answer, we would need to simulate the concentration dependence of the CD spectrum of (−)-**5** using the $\Delta\epsilon$ for each transition and for each species in the equilibrium mixture.[51] Keeping in mind the complexity of the CD spectra of (−)-**5**, just to obtain a value of $\Delta\epsilon$ for all the transitions of (−)-**5** would be an immense and difficult task far beyond the scope of this work. However, one important suggestion from the investigation of the concentration dependence of the CD spectrum of (−)-**5** is that there is no intermolecular interaction between (−)-**5** due to $\pi-\pi$ stacking because there is no new exciton emerging in the CD spectrum on going from the lowest (monomer) to the highest concentration (DP = 2−3). This conclusion is further supported by the di-*N*-benzylated analogue, (−)-**14**, for which the 2-pyridone hydrogen-bonding motif is blocked, thus leaving $\pi-\pi$ stacking as the most probable mode of intermolecular interaction. As stated above, in its CD spectra, the value of $\Delta\epsilon$ shows no concentration dependence, meaning the absence of aggregation and thus no $\pi-\pi$ stacking. Thus when (−)-**14** shows no sign of $\pi-\pi$ stacking, it is unlikely that the congener (−)-**5** should do so.

Conclusions

We have designed a rigid self-aggregating helical tubular structure where chirality and helicity information is encoded in the building blocks, and where both hydrogen bonding and homochiral units constitute the integral part of the helical backbone.[52] More specifically, the synthesis of novel chiral molecular cavity compounds (−)-**4** and (−)-**5**, containing an *all*-carbon bicyclo[3.3.1]nonane skeleton, incorporating the self-complementary hydrogen bonding 2-pyridone motif, in enantiomerically pure forms, has been accomplished.

In the solid state, packing of (−)-**4** into supramolecular networks, more specifically, into columnar stacks interconnected by hydrogen bonds, is assisted by heteroaromatic face−C−H (aliphatic) interactions as revealed by single-crystal X-ray diffraction analysis. Notably, as for the parent compound **3**, the 2-pyridone hydrogen-bonding AD−DA motif fails to operate in the solid state. Instead, the hydrogen-bonded (D−A) chains, ···O═C−N−H···O═C−N−H···O═C−N−H···, interconnecting columnar stacks, comprise helices of right-handed (P) chirality.

In solution, the most probable mode of aggregation of (−)-**5** is as tubular helical structures of various lengths via hydrogen bonding between self-complementary 2-pyridone motifs. This conclusion is supported by the fact that the value of the standard enthalpy of association of (−)-**5** is very similar to the one for the dimerization of 2-pyridone itself, −24.7 kJ mol^{-1}, strongly

(48) Rodger, A.; Nordén, B. *Circular Dichroism & Linear Dichroism*: Oxford University Press: Cambridge, UK, 1999.

(49) Prince, R. B.; Barnes, S. A.; Moore, J. S. *J. Am. Chem. Soc.* **2000**, *122*, 2758−2762.

(50) Ky Hirschberg, J. H. K.; Koevoets, R. A.; Sijbesma, R. P.; Meijer, E. W. *Chem. Eur. J.* **2003**, *9*, 4222−4231.

(51) Forman, J. E.; Barrans, R. E., Jr.; Dougherty, D. A. *J. Am. Chem. Soc.* **1995**, *117*, 9213−9228 and references therein.

(52) The enantiopure 2,2′-dimethylbiphenyl-6,6′-dipropiolic acid and amide are close to this design principle. This molecule forms helices in the solid state: Tichý, M.; Holý, P.; Závada, J.; Císařová, I.; Podlaha, J. *Tetrahedron: Asymmetry* **2001**, *12*, 2295−2300.

suggesting that (−)-**5** also aggregates using its two 2-pyridone AD−DA hydrogen-bonding motifs. This observation together with the fact that (−)-**5** is optically pure and has two 2-pyridone units rigidly attached in a screw-shaped orientation leads to the conclusion that the only possible geometry of the aggregates will be tubular helical. Moreover, the large shift change of the NH proton resonance at different concentrations and temperatures supports the involvement of the 2-pyridone AD−DA hydrogen-bonding motifs in the aggregation of (−)-**5**. The extent of aggregation is limited being, at the most, on an average 11 units in CD_2Cl_2 at 299 K at the highest concentration investigated as seen from the NMR titrations. The second most probable mode of aggregation, $\pi-\pi$ stacking, can be refuted based on NMR spectroscopy and in addition by electronic and CD spectroscopy. The self-association data for (−)-**5** fit the isodesmic indefinite (equal *K*) model of aggregation as demonstrated by NMR titrations and VPO measurements, implying that there is no additional stabilization due to interactions between turns (or part of turns) of each helix. Such a noncooperative mode of propagation of each helical aggregate in the system is supported by molecular modeling of a tubular helix containing monomers of similar type as (−)-**5**, associated by the 2-pyridone AD−DA hydrogen-bonding motif (Figure 2). To the best of our knowledge, this is the first example of a well-characterized helical tubular structure in solution containing a backbone assembled by hydrogen bonds, not stabilized by additional forces, such as $\pi-\pi$ stacking and ionic interactions.

Inspired by the results from the present system, we are now proceeding toward analogues of (−)-**5** assembling via four hydrogen bonds, to obtain aggregates of larger size with the ultimate goal to use the proposed tubular helical structures for capture or even transport of molecules inside the so formed tubes.

Experimental Section

General Remarks. All the chemicals and solvents were used as received form commercial sources without further purification unless noted. The $CDCl_3$ used for the ^{1}H NMR dilution titrations had been stored over Ag. Its water content was estimated to less than 500 ppm based on ^{1}H NMR analysis. The CD_2Cl_2 used for the ^{1}H NMR dilution titrations was dried over 4 Å molecular sieves prior to use. The $CHCl_3$ used for VPO measurements was ethanol free and distilled from powdered 4 Å molecular sieves prior to use. TLC analyses (Merck 60 F254 sheets) were visualized under UV light (254 nm) or with cerium-(IV) sulfate solution. Column chromatography was performed on silica gel (Matrex 0.063−0.200 mm). Melting points (mp) were determined in capillary tubes and were uncorrected. Chiral GC analysis was carried out on a Perkin-Elmer Autosystem instrument using a Beta-Dex 120 fused silica capillary column.

Chemical shifts are given in parts per million relative to TMS using the residual $CHCl_3$ peaks at $\delta = 7.27$ (^{1}H NMR) and 77.16 (^{13}C NMR) ppm in $CDCl_3$ or the residual CH_2Cl_2 peak at $\delta = 5.30$ (^{1}H NMR) ppm in CD_2Cl_2, or the residual DMSO peaks at $\delta = 2.50$ (^{1}H NMR) and 39.5 (^{13}C NMR) in DMSO-d_6 as internal standards. NMR spectra were recorded in $CDCl_3$ unless stated otherwise. For numbering of atoms, see Figure 1. The temperature of the NMR titrations was estimated by measuring the separation between the proton resonances of the OH and the CH_3 group[53] using an NMR tube containing MeOH.

IR spectra were obtained in KBr pellets and are reported in cm^{-1}.

VPO measurements were done with a Knauer K-7000 machine in chloroform solutions at 35 °C using benzil (Knauer) as a standard.

(53) Atkitt, J. W.; Mann, B. E. *NMR and Chemistry: An Introduction to Modern NMR Spectroscopy*, 4th ed.; Stanley Thorns: Glasgow, UK, 2000.

The electronic spectra were recorded on a Varian Cary100 Biospectrophotometer, and the CD spectra were recorded on a Jasco Model J-500A spectropolarimeter using spectral grade 2-propanol or $CHCl_3$. For the UV and CD titrations, CH_2Cl_2 was distilled over CaH_2. In the investigation of the concentration dependence of the UV and CD spectra of (−)-**5** (Figures 11 and 12), a stock solution of (−)-**5** in CH_2Cl_2 (3.3 mM) was used, and less concentrated solutions were prepared by diluting the previous more concentrated one twice. The CD spectra of the prepared seven solutions (including the stock solution) were recorded. For the three most concentrated solutions, the recordings were carried out using a cell of 0.01 cm width and for the others 0.1 cm. UV spectra were measured in a cell of 0.1 cm width.

Optical rotations were measured on a Perkin-Elmer 141 instrument. $[\alpha]^{25}_D$ values are given in 10^{-1} deg cm^{-1} g^{-1}, and concentrations are given in units of g/100 cm^3.

Synthesis. 1-Benzyl-4-hydroxy-6-methyl-2(1*H*)-pyridinone (9). To a stirred suspension of 4-hydroxy-6-methyl-2*H*-pyran-2-one **8** (10.0 g, 0.080 mol) in water (30 mL) was added benzylamine (8.6 g, 0.080 mol) dropwise over a period of 30 min at 100 °C. The reaction mixture was then heated under reflux for 16 h. The reaction mixture was cooled; the solid was filtered, washed with water, and dried in a vacuum desiccator over $CaCl_2$. The crude reaction product was suspended in acetone (70 mL), heated under reflux for 1 h, and filtered. The remaining solid was recrystallized from methanol to afford **3** (8.4 g, 56%) as an off-white solid, mp 215 °C. An analytical sample was obtained after three crystallizations from methanol, mp 216−217 °C (lit. data mp 217 °C[22]).

1-Benzyl-4-(4-tosyloxy)-6-methyl-2(1*H*)-pyridinone (10). A solution of **9** (450 mg, 1.86 mmol) and *p*-toluenesulfonyl chloride (530 mg, 2.78 mmol) in dry pyridine (7.5 mL) was stirred overnight at room temperature. The reaction mixture was diluted with chloroform (40 mL), washed with water, 5% HCl solution, and water. The organic layer was dried, evaporated to dryness, and the remaining solid was purified by flash chromatography ($CHCl_3$) to afford **10** (660 mg, 97%) as a yellowish solid, mp 115 °C; R_f 0.11 ($CHCl_3$); IR ν 1670 (C═O), 1596, 1559, 1379, 1372 (S═O), 1192, 1178, 1118, 1087, 980, 854, 819, 753, 735, 666, 550; ^{1}H NMR (400 MHz) δ 7.81−7.78 (2H, m, H-tolyl), 7.36−7.34 (2H, m, H-tolyl), 7.31−7.22 (3H, m, H−Ph), 7.09−7.07 (2H, m, H−Ph), 6.05−6.03 (2H, m, H-3, 5), 5.25 (2H, s, H-*CH*$_2$Ph), 2.45 (3H, s, H-tolyl-CH_3), 2.24 (3H, s, H−CH_3); ^{13}C NMR (100.6 MHz) δ 164.1 (C-2), 158.1 (C-6), 148.4 (C-4), 146.1 (tolyl), 135.7 (Ph), 132.0 (tolyl), 130.1 (2C, tolyl), 128.9 (2C, tolyl), 128.3 (2C, Ph), 127.5 (Ph), 126.3 (2C, Ph), 107.4 (C-3), 103.0 (C-5), 42.2 (2C, *CH*$_2$−Ph), 21.8 (tolyl-CH_3), 20.8 (CH_3); MS, *m*/*z* (%) 371 ([M + 2]$^+$, 22), 370 ([M + 1]$^+$, 100), 369 ([M]$^+$, 26), 214 (6), 91 (47). Anal. Calcd for $C_{20}H_{19}NO_4S$: C, 65.02; H, 5.18; N, 3.78. Found: C, 65.06; H, 4.94; N, 4.12. HRMS (FAB+) calcd for $C_{20}H_{20}NO_4S$ ([M + H]$^+$) 370.1113, found 370.1115.

1-Benzyl-4-chloro-6-methyl-2(1*H*)-pyridinone (11). A mixture of finely powdered **9** (2.0 g, 9.3 mmol) and $POCl_3$ (1.04 mL, 11.2 mmol) was heated at 80 °C for 40 min. The cooled reaction mixture was dissolved in dichloromethane (100 mL) and washed with water (3 × 20 mL). The organic layer was dried (Na_2SO_4), evaporated to dryness, and the remaining solid was purified by flash chromatography (3:2 heptane/ethyl acetate) to afford **11** (580 mg, 27%) as an off-white solid, mp 87−88 °C; R_f 0.3 (3:2 heptane/ethyl acetate); IR ν 1660 (C═O), 1578, 1548, 1346, 1083, 890, 871, 724, 692; ^{1}H NMR (400 MHz) δ 7.32−7.22 (3H, m, H−Ph), 7.13−7.11 (2H, m, H−Ph), 6.58 (1H, d, J = 2.1 Hz, H-3), 6.07 (1H, dd, J = 2.1 and 0.6 Hz, H-5), 5.28 (2H, s, H-*CH*$_2$Ph), 2.24 (3H, s, CH_3); ^{13}C NMR (100.6 MHz) δ 162.9 (C-2), 147.1 (C-6), 146.3 (Ph), 135.8 (C-4), 128.8 (2C, Ph), 127.5 (Ph), 126.3 (2C, Ph), 116.3 (C-3), 108.5 (C-5), 47.0 (*CH*$_2$−Ph), 20. 5 (CH_3); MS, *m*/*z* (%) 234/236 ([M + 1]$^+$, 100/31), 233/235 ([M]$^+$, 35/22), 154 (12), 136 (13), 91 (77). Anal. Calcd for $C_{13}H_{12}ClNO$: C, 66.81; H, 5.18; N, 5.99. Found: C, 66.48; H, 5.06; N, 6.01. HRMS (FAB+) calcd for $C_{13}H_{13}{}^{35}ClNO$ ([M + H]$^+$) 234.0685, found 234.0684.

1-Benzyl-4-hydrazino-6-methyl-2(1*H*)-pyridinone (7). Method A: To a solution of **11** (540 mg, 2.31 mmol) in methanol (20 mL) was added hydrazine monohydrate (1.12 mL, 23.1 mmol), and the resulting mixture was heated under reflux for 30 h. Cooled reaction mixture was evaporated to dryness, and the remaining solid was purified by flash chromatography (10:1 $CHCl_3$/MeOH) to afford **7** (430 mg, 81%) as a brownish solid, mp 218−220 °C. **Method B:** Finely powdered **9** (100 mg, 0.46 mmol) and hydrazine hydrate (204 μL, 4.2 mmol) were placed into a 15 mL pressure tube (Ace, with Teflon bushing and FETFE O-ring, length 10.2 cm). The reaction tube was placed in a beaker filled with vermiculite and irradiated in an ordinary domestic microwave oven (Zanussi ZM17M with rotate plate) for 6 min at 250 W. The reaction could not be performed in more than ca. 0.5 mmol scale since too high pressure develops and hydrazine hydrate escapes from the reaction vessel. The reaction mixture was cooled, the residue dissolved in methanol, and collected. The procedure was repeated four more times (in total 500 mg, 2.3 mmol of **6**); the combined solutions were evaporated to dryness, and the remaining solid was purified by flash chromatography (10:1 $CHCl_3$/MeOH) to afford **7** (300 mg, 57%) as a brownish solid, mp 218−220 °C; R_f 0.19 (10:1 $CHCl_3$/MeOH); IR ν 3259, 3194 (NH), 1652 (C═O), 1573, 1531, 818, 721; ^{1}H NMR (400 MHz, DMSO-d_6) δ 7.51 (1H, s, NH), 7.33−7.28 (2H, m, H−Ph), 7.25−7.20 (1H, m, H−Ph), 7.08−7.07 (2H, m, H−Ph), 5.61 (1H, bs, H-3), 5.49 (1H, d, J = 2.1 Hz, H-5), 5.13 (2H, s, H-CH_2-Ph), 4.12 (2H, bs, NH), 2.07 (3H, s, H−CH_3); ^{13}C NMR (100.6 MHz, DMSO-d_6) δ 163.8 (C-2), 158.1 (C-4), 145.2 (C-6), 138.8 (Ph), 128.7 (2C, Ph), 126.9 (Ph), 126.3 (2C, Ph), 96.9 (C-3), 87.6 (C-5), 44.9 (2C, CH_2−Ph), 20.2 (CH_3); MS, *m*/*z* (%) 231 ([M + 2]$^+$, 17), 230 ([M + 1]$^+$, 100), 229 ([M − 1]$^+$, 34), 154 (16), 136 (11), 91 (42). HRMS (FAB+) calcd for $C_{13}H_{16}N_3O$ ([M + H]$^+$) 230.1293, found 230.1292.

(1*S*,5*S*)-Bicyclo[3.3.1]nonane-2,6-dione bis[(1-benzyl-6-methyl-2-oxo-1,2-dihydro-4-pyridinyl)hydrazone] 12. Hydrazine **7** (500 mg, 2.19 mmol) and (+)-(1*S*,5*S*)-**2** (150 mg, 1.00 mmol) were dissolved in methanol with heating. The resulting clear solution was refluxed for 5 h. The reaction mixture was cooled, the precipitate was filtered, washed twice with cold solvent, and dried in vacuo to afford the hydrazone as a mixture of *E,E* and *E,Z* isomers, which was used without further purification. Yield 550 mg (95%), white solid, mp >320 °C; IR ν 3418, 3228 (NH), 1643 (C═O), 1564, 1531, 1236, 825; MS, *m*/*z* (%) 575 ([M + 1]$^+$, 23), 307 (47), 298 (18), 154 (100), 136 (74), 107 (22), 91 (28), 89 (22). Anal. Calcd for $C_{35}H_{38}N_6O_2$: C, 73.14; H, 6.66; N, 14.62. Found: C, 72.98; H, 6.58; N, 14.78. HRMS (FAB+) calcd for $C_{35}H_{39}N_6O_2$ ([M + H]$^+$) 575.3134, found 575.3121.

(6*R*,13*R*)-2,9-Dibenzyl-2,9-diaza-3,10-dimethyl-1,8-dioxo-2,5,6,7,9,12,13,14-octahydro-6,13-methanocycloocta[1,2-b:5,6-b′]diindole (6). A round-bottomed flask equipped with an air condenser and rubber septum was charged with hydrazone (1*S*,5*S*)-**12** (500 mg, 0.87 mmol) and diphenyl ether (25 mL). The suspension was stirred and heated at reflux, passing argon through the mixture via a long cannula. After 7.5−8 h, the evolution of ammonia ceased and the reaction mixture was cooled, diluted with pentane, and filtered. The precipitate was washed with diethyl ether and diethyl ether−methanol mixture (1:1 v/v) to give 440 mg (94%) of (6*R*,13*R*)-**6** as a gray solid, mp >320 °C; IR ν 3398, 3281 (NH), 1641 (C═O), 1575; ^{1}H NMR (400 MHz, 11 mg in 0.7 mL of $CDCl_3$/0.02 mL of TFA) δ 10.01 (2H, s, NH), 7.3−7.25 (6H, m, H−Ph), 6.97−6.95 (4H, m, H−Ph), 6.91 (1H, s, H-4(11)), 5.59 (2H, d, ^2J = 16.2 Hz, H−CH_2Ph), 5.47 (2H, d, ^2J = 16.2 Hz, H-CH_2Ph), 3.53 (2H, d, J = 2.6 Hz, H-6(13)), 3.34 (2H, d, ^2J = 16.3 Hz, H_{endo}-7(14)), 3.16 (2H, dd, ^2J = 16.3 Hz, ^3J = 5 Hz, H_{exo}-7(14)), 2.48 (6H, s, H−CH_3), 2.17 (2H, bs, H-15); ^{13}C NMR (100.6 MHz, 11 mg in 0.7 mL of $CDCl_3$/0.02 mL of TFA) δ 156.1 (C-1(8)), 142.1 (C-3(10)), 139.3 (C-4a(11a)), 139.2 (Ph), 134.2 (C-5a(12a)), 129.1 (2C, Ph), 128.1 (Ph), 125.8 (2C, Ph), 111.5 (C-7b(14b)), 110.8 (C-7a-(14a)), 103.9 (C-4(11)), 49.6 (CH_2−Ph), 28.7 (C-6(13)), 28.3 (C-15), 27.4 (C-7(14)), 20.7 (CH_3).

General Procedure for the Alkylation of Methanocyclooctadiindole (6*R*,13*R*)-6. In a round-bottomed flask, NaH (22 mg, 0.56 mmol, 60% dispersion in mineral oil) was washed with dry hexane (2 × 2 mL), and solid (6*R*,13*R*)-**6** (100 mg, 0.185 mmol) was added. The flask was flushed with nitrogen, and dry DMF (25 mL) was added. The reaction mixture was stirred under nitrogen at room temperature until evolution of hydrogen ceased and a clear solution was obtained (ca. 2 h). To the resulting solution were added 1-iododecane (237 μL, 1.1 mmol) or 1-bromodecane (230 μL, 1.1 mmol; together with a catalytic amount of KI) and 1-bromobutane (119 μL, 1.1 mmol; together with a catalytic amount of KI) in dry DMF (1 mL) dropwise, and the mixture was stirred for 24 h. DMF was removed by co-distillation with toluene; the obtained residue was suspended in chloroform and filtered through a short plug of silica gel eluting with chloroform. The filtrate was evaporated to dryness and the residue purified by flash chromatography to afford alkylated methanocyclooctadiindoles.

(−)-(6*R*,13*R*)-2,9-Dibenzyl-5,12-dibutyl-2,9-diaza-3,10-dimethyl-1,8-dioxo-2,5,6,7,9,12,13,14-octahydro-6,13-methanocycloocta[1,2-b:5,6-b′]diindole (13). Yellow solid, yield 69 mg (57%), mp >250 °C (dec); R_f 0.23 (2:3 heptane/ethyl acetate); $[\alpha]_D^{20}$ = −380 (*c* 0.05, $CHCl_3$); UV (in $CHCl_3$), λ_{max} (log ϵ) 318 (4.3, sh), 307 (4.37), 284 (4.26, sh), 231 (4.46); CD (in $CHCl_3$), λ_{max} ($\Delta\epsilon$/dm^3 mol^{-1} cm^{-1}) 322 (−48.99), 310 (−46.65), 288 (0), 282 (7.45), 270 (0), 260 (−5.88). IR: ν 2955, 2928 (CH), 1652 (C═O), 1590; ^{1}H NMR (400 MHz) δ 7.26−7.23 (4H, m, H−Ph), 7.19−7.16 (2H, m, H−Ph), 7.13−7.11 (4H, m, Ph), 6.09 (2H, d, J = 0.6 Hz, H-4(11)), 5.33 (4H, br dd, ^2J = 15.6 Hz, H-CH_2Ph), 4.03 (2H, dt, ^2J = 14.8 Hz, ^3J = 7.5 Hz, H-CH_2N(5,-12)), 3.91 (2H, dt, ^2J = 14.8 Hz, ^3J = 7.5 Hz, H-CH_2N(5,12)), 3.40 (2H, t, ^3J = 2.8 Hz, H-6(13)), 3.31−3.21 (4H, m, H-7(14)), 2.26 (6H, s, H−CH_3), 2.16 (2H, t, J = 2.8 Hz, H-15), 1.73 (4H, quint, ^3J = 7.5 Hz), 1.47−1.34 (4H, m), 0.97 (6H, t, ^3J = 7.4 Hz, H−C_3H_7); ^{13}C NMR (100.6 MHz) δ 160.8 (C-1(8)), 138.2 (C-3(10)), 137.9 (C-4a(11a)), 137.5 (Ph), 134.2 (C-5a(12a)), 128.5 (2C, Ph), 126.69 (Ph), 126.3 (2C, Ph), 112.0 (C-7b(14b)), 111.3 (C-7a(14a)), 94.7 (C-4(11)), 46.0 (CH_2−Ph), 43.3 (C−N(5,12)), 33.1, 30.4 (C-6(13)), 29.1 (C-15), 26.2 (C-7(14)), 21.2, 20.3 (CH_3), 13.8; MS, *m*/*z* (%) 654 ([M + 2]$^+$, 30), 653 ([M + 1]$^+$, 85), 652 ([M]$^+$, 100), 651 ([M − 1]$^+$, 26), 154 (23), 136 (14), 91 (31). Anal. Calcd for $C_{43}H_{48}N_4O_2$: C, 79.11; H, 7.41; N, 8.58. Found: C, 79.31; H, 7.68; N, 8.72. HRMS (FAB+) calcd for $C_{43}H_{48}N_4O_2$ ([M]$^+$) 652.3777, found 652.3787.

(−)-(6*R*,13*R*)-2,9-Dibenzyl-5,12-didecyl-2,9-diaza-3,10-dimethyl-1,8-dioxo-2,5,6,7,9,12,13,14-octahydro-6,13-methanocycloocta[1,2-b:5,6-b′]diindole (14). Yellow glass, yield 126 mg (83%), mp 81−83 °C; R_f 0.22 (7:3 heptane/ethyl acetate); $[\alpha]_D^{20}$ = −244 (*c* 0.073, $CHCl_3$); UV (in CH_2Cl_2), λ_{max} (log ϵ) 319 (4.28, sh), 306 (4.36), 285 (4.23, sh), 220 (4.8, sh); CD (in CH_2Cl_2) λ_{max} ($\Delta\epsilon$/dm^3 mol^{-1} cm^{-1}) 321 (−46.24), 310 (−43.28), 288 (0), 280 (11.86), 267 (0), 257 (−5.93). IR: ν 2925, 2853 (CH), 1654 (C═O), 1590, 729; ^{1}H NMR (400 MHz) δ 7.27−7.23 (4H, m, H−Ph), 7.19−7.16 (2H, m, H−Ph), 7.12−7.11 (4H, m, H−Ph), 6.09 (2H, d, J = 0.5 Hz, H-4(11)), 5.33 (4H, br dd, H−CH_2-Ph), 4.02 (2H, dt, ^2J = 15 Hz, ^3J = 7.5 Hz, H-CH_2N(5,12)), 3.89 (2H, dt, ^2J = 15 Hz, ^3J = 7.5 Hz, H-CH_2N(5,12)), 3.39 (2H, bs, H-6(13)), 3.31−3.21 (4H, m, H-7(14)), 2.26 (6H, s, H−CH_3), 2.15 (2H, bs, H-15), 1.8−1.67 (4H, m), 1.4−1.26 (28H, m), 0.88 (6H, t, ^3J = 7 Hz, H−C_9H_{19}); ^{13}C NMR (100.6 MHz) δ 160.8 (C-1(8)), 138.2 (C-3(10)), 137.9 (C-4a(11a)), 137.5 (Ph), 134.2 (C-5a(12a)), 128.5 (2C, Ph), 126.7 (Ph), 126.4 (2C, Ph), 112.1 (C-7b(14b)), 111.3 (C-7a(14a)), 94.7 (C-4(11)), 46.0 (CH_2−Ph), 43.6 (C−N(5,12)), 31.9, 31.0, 30.4 (C-6(13)), 29.7 (C-15), 29.5, 29.5, 29.3, 29.2, 27.1, 26.3 (C-7(14)), 22.7, 21.3 (CH_3), 14.1; MS, *m*/*z* (%) 822 ([M + 2]$^+$, 40), 821 ([M + 1]$^+$, 88), 820 ([M]$^+$, 100), 819 ([M − 1]$^+$, 35), 429 (10), 339 (9), 91 (51). Anal. Calcd for $C_{55}H_{72}N_4O_2$: C, 80.44; H, 8.84; N, 6.82. Found: C, 80.77; H, 9.09; N, 6.69. HRMS (FAB+) calcd for $C_{55}H_{72}N_4O_2$ ([M]$^+$) 820.5655, found 820.5666.

(−)-(6*R*,13*R*)-5,12-Dibutyl-2,9-diaza-3,10-dimethyl-1,8-dioxo-2,5,6,7,9,12,13,14-octahydro-6,13-methanocycloocta[1,2-b:5,6-b′]di-

indole (4). Methanocyclooctadiindole (−)-**13** (75 mg, 0.011 mmol) in dry THF (6 mL) was added dropwise to liquid ammonia (ca. 18 mL) at −45 °C (dry ice/acetonitrile bath). Sodium was added to the resulting suspension in small pieces until the solution turned dark blue. The reaction mixture was stirred at −45 °C for 6 h, keeping the solution dark blue by addition of sodium. The reaction mixture was quenched by careful addition of excess solid NH_4Cl. After evaporation of ammonia, the residue was suspended in water (10 mL), acidified with 2 M HCl, and extracted with $CHCl_3$. The combined organic phase was dried (Na_2SO_4), evaporated to dryness, and the remaining solid was purified by flash chromatography (95:5 CH_2Cl_2/MeOH) to afford 48 mg (89%) of (−)-**4** as a yellow solid, mp >320 °C (dec); R_f 0.2 (95:5 CH_2Cl_2/MeOH); $[\alpha]_D^{20} = -400$ (*c* 0.0525, $CHCl_3$), UV (*c* 0.11 mM, $CHCl_3$), λ_{max} (log ϵ) 314 (4.26, sh), 303 (4.36), 281 (4.33, sh), 229 (4.41); CD (*c* 1.1 mM, $CHCl_3$), λ_{max} ($\Delta\epsilon$/dm^3 mol^{-1} cm^{-1}) 308 (−32.48), 282 (0), 275 (5.46), 267 (0), 257 (−5.73). IR: ν 3414 (NH), 2957, 2929 (CH), 1638 (C═O), 1459, 1337; ^{1}H NMR (400 MHz, 4.2 mg in 0.7 mL of $CDCl_3$) δ 10.18 (2H, bs, H−NH), 5.96 (2H, s, H-4(11)), 3.98 (2H, dt, ^2J = 14.7 Hz, ^3J = 7.5 Hz, H-*C*H_2N(5,12)), 3.90 (2H, dt, ^2J = 14.7 Hz, ^3J = 7.5 Hz, H-*C*H_2N(5,12)), 3.37 (2H, d, ^3J = 2.5 Hz, H-6(13)), 3.24 (2H, dd, ^2J = 16.3 Hz, ^3J = 4.8 Hz, H_{exo}-7(14)), 3.16 (2H, d, ^2J = 16.3 Hz, H_{endo}-7(14)), 2.23 (6H, s, H−CH_3), 2.12 (2H, br s, H-15), 1.71 (4H, quint, ^3J = 7.8 Hz), 1.44−1.35 (4H, sext, ^3J = 7.3 Hz), 0.98 (6H, t, ^3J = 7.3 Hz, H−C_3H_7); ^{13}C NMR (100.6 MHz, 11 mg in 0.95 mL of $CDCl_3$/0.05 mL of CD_3OD) δ 161.1 (C-1(8)), 140.4 (C-3(10)), 135.2 (C-4a(11a)), 134.5 (C-5a(12a)), 111.2 (C-7b(14b)), 110.7 (C-7a(14a)), 93.7 (C-4(11)), 43.2 (C−N(5,12)), 32.8, 30.0 (C-6(13)), 28.6 (C-15), 25.9 (C-7(14)), 20.1, 18.9 (CH_3), 13.6; MS, *m*/*z* (%) 474 ([M + 2]$^+$, 24), 473 ([M + 1]$^+$, 87), 472 ([M]$^+$, 100), 471 ([M − 1]$^+$, 34), 255 (13). Anal. Calcd for $C_{29}H_{36}N_4O_2$: C, 73.70; H, 7.68; N, 11.85. Found: C, 73.46; H, 7.80; N, 12.10. HRMS (FAB+) calcd for $C_{29}H_{36}N_4O_2$ ([M]$^+$) 472.2838, found 472.2832.

(−)-(6*R*,13*R*)-5,12-Didecyl-2,9-diaza-3,10-dimethyl-1,8-dioxo-2,5,6,7,9,12,13,14-octahydro-6,13-methanocycloocta[1,2-b:5,6-b′]diindole (5). Sodium was added to liquid ammonia (∼25 mL) in small pieces until the dark blue color persists. To the resulting solution was added methanocyclooctadiindole (−)-**14** (25 mg, 0.030 mmol) in dry THF (15 mL) dropwise. After a few minutes, an additional portion of dry THF (10 mL) was added, and the mixture was stirred for 6 h at −45 °C. The reaction mixture was quenched by careful addition of excess solid NH_4Cl. After evaporation of ammonia, the residue was suspended in water (10 mL), acidified with 2 M HCl, and extracted with $CHCl_3$. The combined organic phase was dried (Na_2SO_4), evaporated to dryness, and the remaining solid was purified by flash chromatography (95:5 CH_2Cl_2/MeOH) to afford 16 mg (83%) of (−)-**5** as a yellow glass, mp >220 °C (dec); R_f 0.26 (95:5 CH_2Cl_2/MeOH); $[\alpha]_D^{20} = -222$ (*c* 0.106, $CHCl_3$); UV (*c* 0.4 mM, CH_2Cl_2), λ_{max} (log ϵ) 314 (4.16, sh), 302 (4.28), 279 (4.24, sh), 220 (4.6); CD (*c* 0.4 mM, CH_2Cl_2), λ_{max} ($\Delta\epsilon$/dm^3 mol^{-1} cm^{-1}) 318 (−31.46), 307 (−32.2), 283 (0), 277 (7.77), 268 (0), 258 (−6.29). IR: ν 3419 (NH), 2925, 2853 (CH), 1648 (C═O); ^{1}H NMR (400 MHz, 8.2 mg in 0.7 mL of $CDCl_3$) δ 9.52 (2H, bs, NH), 5.97 (2H, s, H-4(11)), 4.0 (2H, dt, ^2J = 14.8 Hz, ^3J = 7.5 Hz, H-*C*H_2N(5,12)), 3.89 (2H, dt, ^2J = 14.8 Hz, ^3J = 7.5 Hz, H-*C*H_2N(5,12)), 3.37 (2H, d, ^3J = 2.6 Hz, H-6(13)), 3.24 (2H, dd, ^2J = 16 Hz, ^3J = 4.8 Hz, H_{exo}-7(14)), 3.16 (2H, d, ^2J = 16 Hz, H_{endo}-7(14)), 2.24 (6H, s, H−CH_3), 2.12 (2H, bs, H-15), 1.85−1.62 (4H, m,), 1.39−1.2 (28H, m), 0.88 (6H, t, ^3J = 7 Hz, H−C_9H_{19}); ^{13}C NMR (100.6 MHz) δ 161.2 (C-1(8)), 140.0 (C-3(10)), 135.3 (C-4a(11a)), 134.0 (C-5a(12a)), 111.5 (C-7b(14b)), 111.0 (C-7a(14a)), 93.0 (C-4(11)), 43.6, 31.8, 30.9, 30.4 (C-6(13)), 29.7 (C-15), 29.6, 29.5, 29.3, 29.1, 27.1, 26.1 (C-7(14)), 22.6, 19.4 (CH_3), 14.1; MS, *m*/*z* (%) 642 ([M + 2]$^+$, 36), 641 ([M + 1]$^+$, 100), 640 ([M]$^+$, 93), 639 ([M − 1]$^+$, 26), 499 (7), 339 (32), 211 (9). Anal. Calcd for $C_{41}H_{60}N_4O_2$: C, 76.83; H, 9.44; N, 8.74. Found: C, 77.26; H, 9.86; N, 8.44. HRMS (FAB+) calcd for $C_{41}H_{60}N_4O_2$ ([M]$^+$) 640.4716, found 640.4725.

Crystallographic Data Collection and Structure Determination of (−)-4. Crystals suitable for X-ray diffraction analysis were obtained by slow evaporation of a solution of (−)-**4** in CH_3CN. The intensity data sets for (−)-**4**·CH_3CN were collected at 293 K with a Bruker SMART 1000 CCD system[54] using ω-scans and synchrotron radiation at MAXLAB II, Lund, Sweden (λ = 0.8720 Å).[55] CCD data were extracted and integrated using Twinsolve.[56] The structure was solved by direct methods and refined by full-matrix least-squares calculations on F^2 using SHELXTL 5.1.[57] Friedel pairs were merged. Non-H atoms were refined with anisotropic displacement parameters, and hydrogen atoms were constrained to parent sites, using a riding model. The data are more than 99% complete out to θ = 31°.

Crystallographic data for (−)-4·CH_3CN: $C_{31}H_{39}N_5O_2$, M = 513.67, monoclinic, space group $P2_1$, a = 5.3713(11) Å, b = 25.738(5) Å, c = 20.962(4) Å, β = 90.48(3)°, V = 2897.9(10) Å^3, Z = 4, d_{calc} = 1.177 g cm^{-3}, μ = 0.075 mm^{-1}, λ = 0.872 Å, 9966 reflections measured, $wR(F^2)$ = 0.3317, GOF = 1.178 (all data), $R(F)$ = 0.0943 ($I > 2\sigma(I)$). Min/max residual electron density: −0.255/0.434 e/Å^3.

Acknowledgment. Prof. Ulf Berg, Lund University, is acknowledged for fruitful discussions, Prof. Lars-Ivar Elding, Lund University, for linguistic improvements, and the Swedish Research Council as well as the Swedish Institute (New Visby Program) and the Lithuanian Science and Studies Foundation for financial support.

Supporting Information Available: Details on the estimation of thermodynamic self-association parameters and constants for (−)-**5** using NMR titrations, highest number of monomers using VPO titrations, additional UV spectra, CD and UV signals versus concentration, and crystallographic data for (−)-**4** in CIF format. This material is available free of charge via the Internet at http://pubs.acs.org.

JA061160Z

(54) *BrukerAXS, SMART*; Area Detector Control Software, Bruker Analytical X-ray System, Madison, Wisconsin, USA, 1995.
(55) Cerenius, Y.; Ståhl, K.; Svensson, L. A.; Ursby, T.; Oskarsson, Å.; Albertsson, J.; Liljas, A. J. *Synchrotron Radiat.* **2000**, *7*, 203−208.
(56) *TwinSolve* 2004; A Program for the Deconvolution and Processing of Rotation Twins', RigakuMSC Inc. and Prekat AB (c), 1998−2004.
(57) Sheldrick, G. M. *SHELXTL5.1*, Program for structure solution and least square refinement; University of Göttingen, Germany, 1998.